

# Guarantees on Robot System Performance Using Stochastic Simulation Rollouts

Joseph A. Vincent<sup>1\*</sup>, Aaron O. Feldman<sup>1\*</sup>, and Mac Schwager<sup>1</sup>

**Abstract**—We provide finite-sample performance guarantees for control policies executed on stochastic robotic systems. Given an open- or closed-loop policy and a finite set of trajectory rollouts under the policy, we bound the expected value, value-at-risk, and conditional-value-at-risk of the trajectory cost, and the probability of failure in a sparse rewards setting. The bounds hold, with user-specified probability, for any policy synthesis technique and can be seen as a post-design safety certification. Generating the bounds only requires sampling simulation rollouts, without assumptions on the distribution or complexity of the underlying stochastic system. We adapt these bounds to also give a constraint satisfaction test to verify safety of the robot system. Furthermore, we extend our method to apply when selecting the best policy from a set of candidates, requiring a multi-hypothesis correction. We show the statistical validity of our bounds in the Ant, Half-cheetah, and Swimmer MuJoCo environments and demonstrate our constraint satisfaction test with the Ant. Finally, using the 20 degree-of-freedom MuJoCo Shadow Hand, we show the necessity of the multi-hypothesis correction.

**Index Terms**—Probability and Statistical Methods, Optimization and Optimal Control, Motion and Path Planning, Risk-Sensitive Control

## I. INTRODUCTION

It is essential that robots be able to operate safely and successfully under diverse sources of uncertainty, including uncertainty about their own dynamics and state, friction and contact forces, the future motion of other agents, and environment geometry. For example, robot manipulators must interact with objects having uncertain geometries or physical parameters, legged robots must locomote on uncertain terrain, and autonomous vehicles must avoid colliding with other agents whose future trajectories are uncertain. While it is common to have a simulation model reflecting these diverse sources of uncertainty, we rarely have access to closed-form mathematical models, making it difficult to provide rigorous performance and safety guarantees. We address this challenge, presenting statistical performance bounds and safety tests for arbitrary robotic systems given a finite set of trajectory samples from a stochastic simulator.

Performance for stochastic robotic systems is typically quantified with an expected trajectory cost, or with risk-sensitive performance measures such as Value-at-Risk (VaR)

This work was funded by NASA ULI grant 80NSSC20M0163. The first author was also supported on a on a Dwight D. Eisenhower Transportation Fellowship. The second author was also supported by a National Science Foundation Graduate Research Fellowship under Grant No. 2146755.

<sup>1</sup>Department of Aeronautics and Astronautics, Stanford University, Stanford, CA 94305, USA, {josephav, aofeldma, schwager}@stanford.edu

\* denotes equal author contribution

The code associated with this work can be found at [https://github.com/StanfordMSL/performance\\_guarantees](https://github.com/StanfordMSL/performance_guarantees).

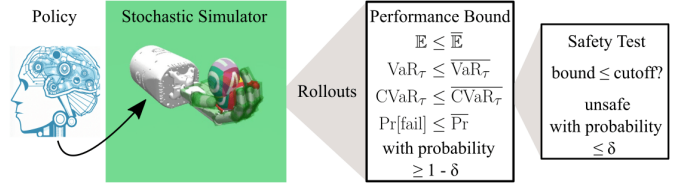


Figure 1. Overview of our method for bounding performance for a single open- or closed-loop policy using a stochastic simulator. The policy is executed in simulation  $n$  times to collect trajectory rollouts. The cost or constraint function is evaluated for each rollout and these samples are used to form a distribution-free upper bound on a given performance measure (expected value, value-at-risk, conditional-value-at-risk, or probability of failure) that is guaranteed to hold with probability at least  $1 - \delta$ . These probabilistic upper bounds may also be used to ensure safety of the policy by testing whether constraints on the performance measures hold. The finite-sample bound guarantee ensures that these tests incorrectly accept a policy as safe with at most  $\delta$  probability. We demonstrate this pipeline for several MuJoCo environments (Ant, Half-Cheetah, and Swimmer) and extend the method to compare multiple policies for manipulating an egg object of uncertain mass and friction with the MuJoCo Shadow Hand.

or Conditional Value-at-Risk (CVaR). Performance can also be quantified by the probability of task success (e.g., probability that an object is not dropped, or a robot does not fall). Symmetrically, safety is often enforced by putting constraints on these performance measures: expected value constraints, VaR constraints, CVaR constraints, or constraints on success probability. We provide probabilistic bounds for all of these performance measures.

Most existing approaches for computing or bounding expected value, VaR, CVaR, or success probability (i) assume a known distribution for the uncertainty (e.g., Gaussian), (ii) use a large number of simulation rollouts to approximate uncertainty without formal guarantees, or (iii) provide formal guarantees that hold asymptotically as the number of samples approaches infinity. In contrast, our methods are both distribution-free (they require no knowledge of the underlying probability distribution), and finite-sample (they hold with a finite number of samples, not just asymptotically). A core insight is that the trajectory cost of the robotic system can be treated as a scalar random variable, and a stochastic simulator can be viewed as an elaborate random number generator, producing independent and identically distributed (IID) samples of the trajectory cost. We can therefore apply distribution-free, finite-sample statistical analysis tools. We only require two key assumptions:

- 1) *The stochasticity in the simulation accurately reflects the uncertainty in the true robot system, and*
- 2) *Successive simulations are IID, that is, there is no mem-*

*ory or distributional shift between trajectory rollouts.*

Specifically, we derive simple formulas using foundational statistical principles to compute upper bounds on expected value, VaR, and CVaR, as well as an upper bound on the probability of failure in a binary success/failure reward model. These bounds are probabilistic, that is, they are allowed to be wrong  $\delta$  proportion of the time, for a user-specified error rate  $\delta$ . We further adapt these bounds to give constraint satisfaction tests for expected value, VaR, CVaR, and failure probability, with a guaranteed user-specified false positive rate (declaring the system safe, when it is actually unsafe). An overview of our method for bounding performance and testing constraint satisfaction for a policy is shown in Fig. 1. We also modify the bounds so they can be used to compare performance among multiple policies, as outlined in Fig. 5. Notably, we show that a multi-hypothesis correction is required to retain statistical guarantees when comparing multiple policies. We empirically demonstrate the validity of our bounds and constraint satisfaction tests in several MuJoCo [1] environments simulated in Gymnasium [2], and verify our policy comparison bounds in a 20 degree-of-freedom MuJoCo Shadow Hand simulation manipulating an object with uncertain mass and friction.

Our bounds are independent of the system’s complexity or dimensionality. They only depend on the number of rollouts and the user-specified error rate. Therefore, our method is appropriate for complex simulation models of high degree-of-freedom robots, featuring, e.g., discontinuities from contact, uncertainties in friction or reaction forces, fluidic or finite-element simulations for soft robots and deformable objects, and aerodynamic simulations for aerial robots. The bounds also apply regardless of how the simulation is derived, applying also when the simulation itself is learned (e.g, generative world models or multi-agent trajectory forecasters). The “simulation” can also be an experimental setup in which a control policy is repeatedly executed on a physical robot. Furthermore, our bounds are valid for open- or closed-loop policies, as well as deterministic or stochastic policies.

We emphasize that we do not present a new policy optimization or planning technique in this work, but rather present a statistical method for bounding the performance of a given control policy or comparing performance among a set of policies. Our methods can be used as a verification tool to bound the performance or certify the safety of a policy obtained from any upstream optimizer (e.g., a reinforcement learning or optimal control design technique or even a large language model task planner).

In summary, our primary contributions are

- 1) Given an open- or closed-loop control policy, we obtain probabilistic upper bounds for expected value, VaR, CVaR, and probability of task failure, from a finite set of simulated trajectory rollouts.
- 2) Similarly, we obtain a probabilistic test to verify the satisfaction of constraints on expected value, VaR, CVaR, or probability of failure. The test has a user-specified false acceptance rate.
- 3) We describe a necessary multi-hypothesis correction to these performance bounds in the case of choosing the best among a finite set of candidate policies.

- 4) We achieve the above for an arbitrarily complex simulator, learned or model-based, with diverse sources of uncertainty, and with any upstream policy generation or optimization approach. As evidence to this, we demonstrate our approach in several MuJoCo environments including with the 20 degree-of-freedom Shadow Hand.

The paper is organized as follows. We give related work in Section II. In Section III we introduce our notation and define the problem setting. In Section IV we present the distribution-free performance bounds and derive constraint satisfaction tests. We empirically validate the bounds and constraint tests in MuJoCo simulations in Section V. In Section VI we introduce the multi-hypothesis correction required when comparing bounds among multiple policies, and demonstrate the validity of this correction in Section VII in simulations with the MuJoCo Shadow Hand manipulating an uncertain object. We offer concluding remarks in Section VIII, and give proofs of theorems and computational details of the simulation examples in the Appendix.

## II. RELATED WORK

### A. Sample-Based Performance Quantification

We build on an emerging literature that uses finite samples from simulation rollouts to produce and optimize for distribution-free guarantees on system performance. Using results from randomized optimization, the authors of [3] construct distribution-free bounds on the VaR of a given robustness metric for a robotic system. Their bound on the VaR is a special case of our bound given in Theorem 1. Similar methods are used in [4] to verify safety and robustness of a reinforcement learning policy and in [5] to place probabilistic bounds on the error of a simulated model.

The authors of [6] use distribution-free statistics to place bounds on coherent risk measures (such as CVaR) and on the quality of optimization via random search. They use these results to formulate a method that randomly searches over policies and chooses the one with the least upper bound on risk. In [7], the same bounds are used to find a nonlinear control plan that is better than a specified percentage of plans. As we show in this work, when policy cost is not deterministic, optimizing for the sample-based bound requires a multi-hypothesis correction to retain validity. This is a crucial step in the policy synthesis process that our paper addresses in Section VI.

The authors of [8] perform verification of closed-loop stochastic systems. Like us, they take a distribution-free finite-sample approach, but with some key differences. While they are primarily interested in verifying closed loop systems with neural network controllers, we take a broader view to systems which need not be differentiable, continuous, or defined in closed form. [8] also discusses choosing the least risky controller from a set of controllers but fails to note the need for a multi-hypothesis correction. Lastly, we use a tighter VaR bound not based on the Dvoretzky–Kiefer–Wolfowitz (DKW) inequality [9, 10] and take a different approach to constraints; we provide analysis for handling a variety of risk-sensitive constraints whereas [8] focuses on signal-temporal logic (STL) constraints.

## B. Risk-Sensitive Control

Our method can be used to certify control policies obtained from existing risk-sensitive control design techniques. We classify the approaches for risk-sensitive control into three broad categories: parametric, distributionally robust, and sampling-based.

In the parametric category are works imposing distributional and structural assumptions to efficiently quantify risk. The authors of [11] compute risk averse policies (in the sense of CVaR) for finite state and action Markov Decision Processes (MDPs) by solving a surrogate MDP. The authors of [12] synthesize a CVaR-safe controller for linear systems using barrier functions. [13] enforces obstacle avoidance chance constraints assuming a Gaussian dynamics disturbance. While parametric approaches provide efficient mechanisms for quantifying and mitigating risk, we avoid the associated assumptions (i.e., on the dynamics or uncertainty distribution), so that our approach can be applied as a general certification step for arbitrary, complex systems.

Instead of assuming a particular uncertainty distribution, some work adopts a distributionally robust approach. The authors of [14] and [15] propose CVaR constrained control where the CVaR is first estimated empirically. Then, based on a known ambiguity set for the disturbance distribution (using the Wasserstein metric) about the empirical CVaR, distributionally robust CVaR constraints are enforced at runtime. The authors of [16] add a constraint on the entropic value at risk (EVaR) in their MPC formulation using its dual representation as the worst-case expectation within a KL divergence-based ambiguity set. These approaches address a slightly different problem from our method: uncertainty mismatch. In our setting, we still assume that our simulator provides samples from the true uncertainty distribution, but our bounds do not require knowledge of that distribution.

Sampling-based approaches use repeated draws of empirical performance to estimate the risk without imposing distributional assumptions. In [17] each agent in a team estimates its VaR using the empirical quantile of recently observed rewards. The authors of [18] impose a CVaR constraint during policy optimization by rewriting the CVaR as a tail expectation so that it can be approximated from rollouts. During MPC, [19] and [20] repeatedly rollout controls under the stochastic dynamics and optimize for the sequence minimizing the average associated trajectory cost.

[21] shows that, under certain conditions, the sample average solution becomes asymptotically optimal (as the number of drawn samples approaches infinity). However, in this work we are interested in producing finite-sample performance guarantees. [22] applies [21] to CVaR-constrained trajectory optimization and provides a finite-sample bound on the CVaR constraint. However, they leverage concentration inequalities which hold uniformly across all controls. Our bounds hold pointwise, necessitating a multi-hypothesis correction, but when comparing only a modest number of policies this can yield tighter guarantees. In summary, while sampling-based control provides context for our work, we are interested in augmenting such methods with finite-sample, distribution-free

statistical guarantees.

## C. Conformal Prediction

Conformal prediction (CP) is increasingly being used for producing distribution-free guarantees in robotics. Given exchangeable data (a weaker condition than IID) and a scoring function, CP produces a confidence interval on the score of a new data sample [23]. In this work, we adapt analysis tools from conformal prediction to obtain our VaR bound, and to assess chance constraint satisfaction. Similar to our work, several papers applying CP to robotics have viewed full robot trajectories as one sample. The authors of [24] use collected data of unsafe trajectories to augment robotic fault-detection systems, achieving a guaranteed false negative rate. In [25], the authors use CP to augment learned forecasting models (e.g., predicting pedestrian motion) with a confidence set of possible trajectories. In [26] the authors use adaptive conformal prediction to now adapt their confidence sets using online data. As in much of the CP robotics literature, we also view trajectories as the fundamental sample to get IID data. However, instead of using offline data, we evaluate performance using a generative stochastic simulator.

## D. Concentration Bounds

Key to our approach is the use of sampling-based distribution-free concentration bounds for risk measures as this allows us to produce rigorous performance guarantees when planning with any arbitrarily complex simulator.

Concentration bounds for CVaR were first given by [27], further refined by [28], and later improved upon by [29]. Each of these results requires bounds on the support of the random variable. Later, [30] provided concentration bounds in the case the random variable is sub-Gaussian or sub-exponential (weaker than boundedness by Hoeffding’s Lemma [31]) which were improved upon in [32]. The CVaR bound we use in this paper is from [29], but we express it in a simpler form and give an accompanying proof. We then extend this bound to give a novel bound on expected value.

Unlike CVaR bounds, VaR bounds place no finite support or sub-Gaussianity restrictions. VaR bounds are often derived via the DKW inequality [30, 33, 34]. Although some authors claim these bounds as contributions to the field, an optimal VaR bound has been available since 2005 [35] (although this optimal VaR bound is derived for continuous random variables, it can be extended for discontinuous random variables using the methods of [36]). In this work we use a slightly suboptimal VaR bound because of its simple form and derivation which we present in the Appendix. The VaR bound we use is well-established in the statistics community, dating back to 1945 (see [36, 37]), but its application to bounding policy performance is new. This classical bound is seemingly unknown to many practitioners and is strictly better than the bounds given in [30, 33].

Concentration bounds on the expected value are more studied than for the VaR or CVaR. Hoeffding’s inequality is arguably the most influential bound of this sort [31] although the bounds given later by Anderson are no worse and often

better [38]. More modern work has focused on bounds which are not defined in closed form [39], and concentration sequences [40]. In this paper we derive a novel, closed-form expectation bound using the CVaR bound we present.

Lastly, confidence intervals for the probability of success parameter in the Bernoulli distribution (often called binomial confidence intervals) have been studied extensively. Unlike other concentration bounds, the majority of methods for binomial confidence intervals are not guaranteed to hold with a user-defined probability, also called the *coverage level* (e.g., Wald, Wilson, Jeffreys', Agresti-Coull, etc. as described in [41, 42]). Methods guaranteed to meet the desired coverage level include those by Clopper and Pearson [43], Sterne [44], Crow [45], Eudey [46, 47], and Stevens [48]. Of these approaches, only the bounds from Eudey and Stevens return confidence intervals with exactly the desired coverage and they do so by inverting randomized hypothesis tests. We show that the confidence interval we derive in Theorem 4 is analogous to the one-sided Clopper-Pearson interval, which is known to be unimprovable amongst non-randomized approaches [49].

### III. PROBLEM SETTING

Here we introduce notation and formalize the problem of quantifying performance and safety for a stochastic robotic system. For a given time horizon  $T$ , we consider either an open-loop policy as a sequence of control actions  $(U_0, \dots, U_{T-1})$ , or a closed-loop policy as a mapping (deterministic or stochastic) from state to action  $U_t \sim \pi_t(X_t)$ . We use the term policy to describe all of these cases, and cover all cases with the notation  $\mathcal{U}$  to represent the stochastic sequence of control actions obtained by executing the policy in simulation. When executing the policy, the control actions drive state evolution from a random starting state  $X_0$  via stochastic dynamics  $F_t$

$$X_0 \sim \mathcal{X}_0 \quad (1a)$$

$$X_{t+1} \sim F_t(X_t, U_t) \quad t = 0, \dots, T-1. \quad (1b)$$

We do not assume access to an explicit functional form or distribution for  $F_t$ , but instead we assume we can sample  $X_{t+1} \sim F_t(X_t, U_t)$  IID from a simulation of the system. We write the stochastic state trajectory as  $\mathcal{X} = (X_0, \dots, X_T)$ , similarly to the control policy  $\mathcal{U}$ . The trajectory cost  $J$  associated with a policy and a state sequence realization is composed of stage-wise costs  $c_t$  as

$$J(\mathcal{X}, \mathcal{U}) = c_T(X_T) + \sum_{t=0}^{T-1} c_t(X_t, U_t). \quad (2)$$

As an important alternative case, we also consider the sparse reward setting often seen in reinforcement learning. We let  $J = 1$  denote task failure and  $J = 0$  denote task success, to keep the interpretation of  $J$  as a cost rather than a reward.

In addition to a cost function, we also consider a constraint function  $g$  which may be used to impose trajectory constraints for safety (such as avoiding collisions, or avoiding control input limits), or for task success (such as not dropping an object, not falling down, or attaining a discrete goal). We

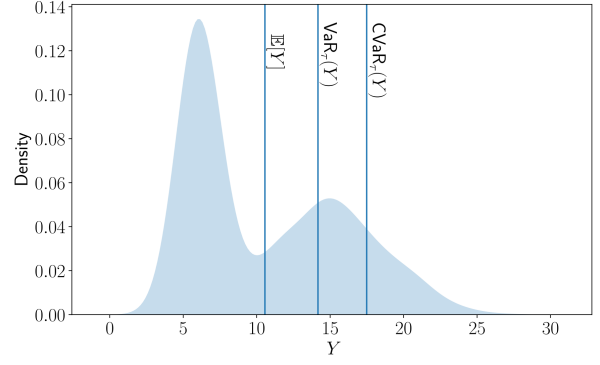


Figure 2. Visualization of the expected value,  $\text{VaR}_\tau$ , and  $\text{CVaR}_\tau$  for an example distribution. Classic stochastic optimal control and reinforcement learning both seek to minimize the expected value of the total cost distribution. Risk-sensitive stochastic optimal control and reinforcement learning consider other measures of performance, such as VaR or CVaR of the cost.

consider the generated trajectory a success when it satisfies a given set of trajectory constraints,

$$g(\mathcal{X}, \mathcal{U}) \leq 0. \quad (3)$$

The above constraint also applies in the binary success/failure setting, in which case  $g = 0$  is task success and  $g = 1$  is task failure, again with the convention of lower  $g$  being safer.

Though the policy is fixed, the associated cost  $J$  and constraint function  $g$  evaluate to random values due to the stochastic dynamics, which generate different state sequence realizations on different runs under the same policy. Therefore, to measure system performance, or to impose safety constraints, we must define a summarizing statistic over the cost or constraint functions, which we call a performance measure.

#### A. Performance Measures

Consider a scalar random variable  $Y$ , representing either the value of the cost function  $J$  or the constraint function  $g$ . We define a performance measure  $\mathcal{P}(Y)$  as a summary statistic for the random variable  $Y$ . The most common choice of performance measure is the expected value  $\mathcal{P}(Y) = \mathbb{E}[Y]$ . However, to be more conservative, we often consider alternative measures that are risk-sensitive, such as the VaR or CVaR of the trajectory cost. VaR, expected value, and CVaR are defined below, and visualized in Fig. 2. Alternatively, in the binary success/failure setting, the probability of failure is the natural performance measure to be minimized. In this work, we consider finite-sample methods for upper bounding all of these quantities.

Recall the cumulative distribution function (CDF), which exists for any scalar random variable, whether continuous or not, is defined as  $\text{CDF}(y) := \Pr[Y \leq y]$ . We define  $\text{VaR}_\tau(Y)$  in terms of the CDF as

**Definition 1** (Value-at-Risk). *Given a scalar random variable  $Y$ , the value at risk of  $Y$  at quantile  $\tau \in (0, 1)$  is*

$$\text{VaR}_\tau(Y) := \inf\{y \mid \text{CDF}(y) \geq \tau\}. \quad (4)$$

If  $Y$  has an invertible CDF then

$$\text{VaR}_\tau(Y) = \{y \mid \text{CDF}(y) = \tau\} = \text{CDF}^{-1}(\tau). \quad (5)$$

In plain words,  $\text{VaR}_\tau = y$  ensures that  $\tau$  proportion of the probability mass of the random variable  $Y$  is below the value  $y$ . The VaR can be seen as a generalization of the inverse of the CDF.

Recall the standard definition of the expected value of a continuous scalar random variable is  $\mathbb{E}[Y] = \int_{-\infty}^{\infty} yp(y) dy$ , where  $p(y)$  is the probability density function. In fact, a more general definition of the expected value can be stated in terms of the  $\text{VaR}_\tau$  as follows,

**Definition 2** (Expected Value). *Given scalar random variable  $Y$ , the expected value of  $y$  is*

$$\mathbb{E}[Y] := \int_0^1 \text{VaR}_\tau(Y) d\tau. \quad (6)$$

The above definition applies to any scalar random variable (continuous, discrete, or mixed). In the case of a continuous random variable with invertible CDF, one can recover the standard definition through a change of variables<sup>1</sup>  $\tau = \text{CDF}(y)$ .

One criticism of VaR as a risk-sensitive performance measure is that it ignores high-cost outcomes that may lie in the  $1-\tau$  tail of the distribution. Conditional Value-at-Risk (CVaR), defined below, addresses this concern.

**Definition 3** (Conditional Value-at-Risk). *Given scalar random variable  $Y$  and  $\tau \in [0, 1)$ , the conditional value at risk of  $Y$  at quantile  $\tau$  is*

$$\text{CVaR}_\tau(Y) := \frac{1}{1-\tau} \int_\tau^1 \text{VaR}_\gamma(Y) d\gamma. \quad (7)$$

If  $Y$  has an invertible CDF then

$$\text{CVaR}_\tau(Y) = \mathbb{E}[Y \mid Y \geq \text{VaR}_\tau(Y)]. \quad (8)$$

There are several equivalent definitions for  $\text{CVaR}_\tau(Y)$ . We prefer the one above as it applies to all scalar random variables (continuous, discrete, or mixed), and it highlights the clear relationship between  $\text{VaR}_\tau(Y)$  and  $\mathbb{E}[Y]$ . We can see that  $\text{CVaR}_\tau(Y)$  is simply the expected value of  $Y$  taken over the top  $1-\tau$  tail of the probability mass (and re-normalized by  $1-\tau$  to ensure it remains a valid expectation). Taking  $\tau = 0$  recovers the expected value. In contrast to  $\text{VaR}_\tau$ ,  $\text{CVaR}_\tau$  captures high-cost tail events. It therefore incorporates the worst case cost situations, and is often quite conservative.  $\text{CVaR}_\tau(Y)$  is always greater than or equal to both  $\mathbb{E}[Y]$  and  $\text{VaR}_\tau(Y)$ . However,  $\mathbb{E}[Y]$  and  $\text{VaR}_\tau(Y)$  may lie in either order, depending on the quantile  $\tau$  and the distribution of the random variable  $Y$ .

For simple distributions (e.g., Gaussians)  $\mathbb{E}[Y]$ ,  $\text{VaR}_\tau(Y)$ , and  $\text{CVaR}_\tau(Y)$  can be found. However, in more realistic robotics scenarios, distributions are non-Gaussian and usually are unknown, so none of these performance measures can be

obtained in closed form. This motivates the need in this paper to give finite-sample bounds for these quantities.

We next formalize the probability of failure as a performance measure for problems with binary success/failure reward models.

**Definition 4** (Failure Probability). *Given a Bernoulli random variable  $Y$ , we refer to  $q = \Pr[Y = 1]$  as the failure probability.*

Note that failure probability is actually a special case of expected value, since  $\Pr[Y = 1] = \mathbb{E}[Y]$  for a binary random variable  $Y$ . However, the binary case allows for significantly tighter bounds than the general bounds on expected value. We therefore treat this case separately.

#### B. Cost Performance and Safety Performance

The performance measures above can be applied to the cost function  $\mathcal{P}(J)$  to measure cost performance, or to the constraint function  $\mathcal{P}(g)$  to measure safety performance. In this paper, we present bounds  $\bar{P}$  to probabilistically bound the cost performance from a finite set of simulation rollouts. Specifically, we give bounds of the form

$$\Pr[\mathcal{P}(J) \leq \bar{P}] \geq 1 - \delta, \quad (9)$$

where  $\delta$  is a user-defined error rate for the bound.

Similarly, safety is often quantified by putting constraints on a performance measure applied to the constraint function,  $\mathcal{P}(g) \leq C$ , for some constant  $C$ . Specifically, one might consider safety as a bound on any of the above performance measures,

$$\mathbb{E}[g] \leq C_{\mathbb{E}}, \quad (10a)$$

$$\text{VaR}_\tau(g) \leq C_{\text{VaR}}, \quad (10b)$$

$$\text{CVaR}_\tau(g) \leq C_{\text{CVaR}}, \quad (10c)$$

$$\Pr[g = 1] \leq C_q. \quad (10d)$$

where in (10d) we consider the case where  $g$  is assumed to be binary with  $g = 1$  indicating failure.

The above formulation in (10) already captures chance constraints (as seen in stochastic optimal control) which require that the trajectory constraint (3) be satisfied with sufficiently high probability. This follows because constraining  $\text{VaR}_\tau(g)$  in (10b) is equivalent to imposing a chance constraint on  $g$ ,

$$\text{VaR}_\tau(g) \leq 0 \iff \Pr[g \leq 0] \geq \tau. \quad (11)$$

In fact, chance constraints can also be modeled as a binary success/failure of the type (10d), where  $g = 1$  denotes the event that the trajectory fails the constraint (3), and  $g = 0$  for a successful trajectory satisfying the constraint.

Notice we cannot directly evaluate whether or not the constraints in (10) hold, because we cannot compute their left hand side when we only have access to a simulator. We therefore define a test for whether  $\bar{P} \leq C$ , using the finite-sample bound  $\bar{P}$ . If  $\bar{P}$  passes this test, we declare the constraint satisfied. In the following section we prove that such a test can be constructed with a user-specified false positive error rate, only concluding an unsafe policy is safe some small fraction of the time.

<sup>1</sup>With the change of variables  $\tau = \text{CDF}(y)$ , we have  $d\tau = p(y) dy$  (recalling that  $p(y) = d\text{CDF}(y)/dy$ ). The domain of integration  $\tau \in (0, 1)$  becomes  $y \in (-\infty, \infty)$ , and since  $\text{VaR}_\tau(Y) = \text{CDF}^{-1}(\tau)$ , the integrand becomes  $\text{CDF}^{-1}(\text{CDF}(y)) = y$ , leading to  $\int_{-\infty}^{\infty} yp(y) dy$ .

#### IV. FINITE-SAMPLE PERFORMANCE BOUNDS

In this section we provide finite-sample upper bounds for the expected value, VaR, CVaR, and failure probability. We also define constraint satisfaction tests based on these bounds. We require access to IID samples of the total cost  $J$  or constraint function  $g$  under the policy being evaluated, which we assume are obtained from a stochastic simulator of the robot system. Each bound presented holds probabilistically, with probability  $1 - \delta$ , where the randomness stems from the bound itself being a function of a finite set of random samples. In fact, if no distributional assumptions are made, one can only formulate bounds that hold probabilistically (see Section 5 of [50]). We refer to  $\delta$  as the user-specified error rate for the bound. All proofs are deferred to the Appendix. An overview of the method is shown in Fig. 1.

As explained previously, our results rest upon two foundational assumptions.

**Assumption 1** (Accurate Simulation Model). *The simulation in (1a), (1b) accurately reflects the true stochastic robot system.*

**Assumption 2** (IID). *Successive simulations are independent and identically distributed, that is, there is no memory or distributional shift between trajectory rollouts.*

Of course, these assumptions will never exactly hold in practice, as there is always some sim-to-real gap. However, qualitatively, the closer the simulation model is to the real robotic system, the more reliable the bounds will be.

##### A. Performance Bounds

The bounds make use of the concept of order statistics, defined as follows.

**Definition 5** (Order Statistics). *For a set of  $n$  samples  $J_{1:n}$  drawn IID, we let  $J_{(k)}$  denote the  $k$ th order statistic, obtained by arranging the samples in order from smallest to largest and taking the  $k$ th element in the sequence.*

**Definition 6** (Binomial Distribution). *Let  $\text{Bin}(k; m, p)$  denote the Binomial cumulative distribution function, with  $m$  trials, success probability  $p$ , evaluated at  $k$  successes.*

**Theorem 1** (VaR Bound). *Consider  $\tau, \delta \in (0, 1)$  and  $n$  IID cost samples  $J_{1:n}$ , and let  $k$  be the smallest index such that  $\text{Bin}(k - 1; n, \tau) \geq 1 - \delta$ . We have the following probabilistic upper bound on  $\text{VaR}_\tau(J)$ ,*

$$\overline{\text{VaR}}_\tau := J_{(k)}, \quad (12)$$

which has the property

$$\Pr[\text{VaR}_\tau(J) \leq \overline{\text{VaR}}_\tau] \geq 1 - \delta.$$

A feasible value for  $k$  exists when  $n \geq \lceil \ln(\delta) / \ln(\tau) \rceil$ , i.e.,  $n$  is large enough to ensure  $\text{Bin}(n - 1; n, \tau) \geq 1 - \delta$ .

*Proof:* The proof for this as well as for lower bounds and two-sided bounds are given in the Appendix. ■

The VaR bound above simply chooses one of the order statistics based on a test involving the cumulative binomial

distribution. Its proof (in the Appendix) is inspired by similar analyses in Conformal Prediction [23, 51]. In our experience, this bound is considerably tighter than other VaR bounds in the recent literature (e.g., [30, 33]), and tends to be tighter in practice than the CVaR and  $\mathbb{E}$  bounds below. As previously stated, the form of this bound is well known in the statistics literature [36, 37], but its application to bounding policy performance is new. The VaR bound in [6] is a special case of this one, which considers the bound arising from the largest order statistic,  $J_{(n)}$ .

Before stating the CVaR and  $\mathbb{E}$  bounds, we require an additional assumption.

**Assumption 3** (Almost Sure Upper Bound). *We have an almost sure upper bound  $J_{\text{ub}}$  such that  $\Pr[J \leq J_{\text{ub}}] = 1$ .*

It may seem circular to require one upper bound in order to produce another upper bound. The idea is to combine the order statistics  $J_{(i)}$  with the almost sure upper bound to produce a significantly tighter bound. In fact, any finite sample upper bound on CVaR or  $\mathbb{E}$  requires knowledge of such an *a priori* known bound on the right tail of the distribution of  $J$ . Two common choices are an almost sure upper bound (as we assume here) or a sub-Gaussian assumption. Without such a tail bound one can adversarially construct a distribution that violates any claimed CVaR or  $\mathbb{E}$  bound by placing a finite probability mass arbitrarily far to the right in the distribution, pulling both CVaR and  $\mathbb{E}$  far enough right to violate the claimed bound. By contrast VaR ignores the tail, so finite sample bounds on VaR can be constructed without a priori bounds on the tail.

Since  $J$  is computed as the sum of  $T$  stage costs it suffices to simply find bounds on the stage cost and multiply these by  $T$  to bound the trajectory cost. For some cost functions bounds may be computed analytically, especially in the case of bounded state and control spaces. Otherwise, in practice one can always clip the value of the cost function between some user-defined bounds, bounding the support of the total cost by construction. Computation of support bounds can be done offline and tight support bounds are not needed, but tighter support bounds on  $J$  will lead to tighter bounds on  $\mathbb{E}[J]$  and  $\text{CVaR}_\tau(J)$ .

Finally, we define a constant that arises in both CVaR and  $\mathbb{E}$  bounds, originating from the application of the DKW bound [9, 10] in their derivation, as discussed in the proofs in the Appendix.

**Definition 7** (DKW Gap). *We define the DKW gap as*

$$\epsilon(\delta, n) = \sqrt{\frac{-\ln \delta}{2n}}.$$

**Theorem 2** (Expected Value). *Consider  $\delta \in (0, 0.5]$ , an almost sure upper bound  $J_{\text{ub}}$ , and  $n$  IID cost samples  $J_{1:n}$ . Let  $k$  be the smallest index such that  $\frac{k}{n} - \epsilon \geq 0$ . We have the following probabilistic upper bound on  $\mathbb{E}[J]$ ,*

$$\overline{\mathbb{E}} := \epsilon J_{\text{ub}} + \left( \frac{k}{n} - \epsilon \right) J_{(k)} + \frac{1}{n} \sum_{i=k+1}^n J_{(i)}, \quad (13)$$



which has the property

$$\Pr[\mathbb{E}[J] \leq \overline{\mathbb{E}}] \geq 1 - \delta.$$

We require the number of samples  $n \geq -\frac{1}{2} \ln(\delta)$ , to ensure  $\epsilon \leq 1$ . If  $k = n$ , the summation on the right is ignored. For  $n < -\frac{1}{2} \ln(\delta)$  we default to the almost sure bound  $J_{ub}$ .

*Proof:* The proof for this as well as for lower bounds and two-sided bounds are given in the Appendix. ■

**Theorem 3 (CVaR Bound).** Consider  $\tau \in [0, 1)$ ,  $\delta \in (0, 0.5]$ , an upper bound  $J_{ub}$ , and  $n$  IID cost samples  $J_{1:n}$ . Let  $k$  be the smallest index such that  $\frac{k}{n} - \epsilon - \tau \geq 0$ . We have the following probabilistic upper bound on  $\text{CVaR}_\tau$ ,

$$\overline{\text{CVaR}}_\tau := \frac{1}{1 - \tau} \left[ \epsilon J_{ub} + \left( \frac{k}{n} - \epsilon - \tau \right) J_{(k)} + \frac{1}{n} \sum_{i=k+1}^n J_{(i)} \right], \quad (14)$$

which has the property

$$\Pr[\text{CVaR}_\tau(J) \leq \overline{\text{CVaR}}_\tau] \geq 1 - \delta.$$

We require the number of samples  $n \geq -\frac{1}{2} \ln(\delta)/(1 - \tau)^2$ , to ensure  $\epsilon \leq 1 - \tau$ . If  $k = n$ , the sum on the right is ignored. For  $n < -\frac{1}{2} \ln(\delta)/(1 - \tau)^2$  we default to the almost sure bound  $J_{ub}$ .

*Proof:* The proof for this as well as for lower bounds and two-sided bounds are given in the Appendix. ■

Both the CVaR and  $\mathbb{E}$  bounds above take the form of a sample average over the order statistics, excluding some proportion of the smaller order statistics defined by the DKW gap  $\epsilon(\delta, n)$ , and including the upper bound  $J_{ub}$  and the smallest effective order statistic  $J_{(k)}$  with special weightings, also determined by  $\epsilon(\delta, n)$ . Therefore, both of these bounds can be understood as variations on the sample average that typically serves as a proxy for expected value. The great advantage of these bounds is that, unlike a sample average, they rigorously upper bound the unknown quantity (CVaR or  $\mathbb{E}$ ) with a user-defined probability  $1 - \delta$  without knowing the underlying probability distribution of  $J$ .

Notice that setting  $\tau = 0$  in the CVaR bound gives the  $\mathbb{E}$  bound, which is appealing given that this is also true of CVaR and  $\mathbb{E}$  from their definitions in Def. 3 and Def. 2 above. While, to our knowledge, these bounds have not previously appeared in the literature, we note that the CVaR bound in Theorem 3 is mathematically equivalent to the one derived in [29], but expressed in a different form and derived by different means.

Finally, we introduce an upper bound on the probability of failure in a binary cost setting.

**Theorem 4 (Failure Probability Bound).** Given  $\delta \in (0, 1)$  and  $n$  IID Bernoulli samples  $J_{1:n}$  (where  $J = 1$  denotes failure) with  $k = n - \sum_{i=1}^n J_i$  successes, we have the following probabilistic upper bound on the probability of failure,  $q := \Pr[J = 1]$ ,

$$\bar{q} = 1 - \min\{p' \in [0, 1] \mid \text{Bin}(k - 1; n, p') \leq 1 - \delta\}, \quad (15)$$

which has the property

$$\Pr[q \leq \bar{q}] \geq 1 - \delta.$$

*Proof:* See the Appendix. ■

## B. Constraint Satisfaction Tests

The above theorems bound performance measures on the random cost  $J$  attained by a robotic system under a given control policy. Now we adapt the above bounds to give a test for constraint satisfaction. Consider any of the performance measures above applied to the constraint function,  $\mathcal{P}(g)$ , embedded in a constraint

$$\mathcal{P}(g) \leq C.$$

Using the associated finite-sample bound, which we write generically as  $\bar{P}$ , we define the associated constraint test as  $\bar{P} \leq C$ . We have the following result.

**Theorem 5 (Constraint Test).** The test for constraint satisfaction  $\bar{P} \leq C$  has a false positive rate of no more than  $\delta$ , that is,

$$\Pr[\bar{P} \leq C \mid \mathcal{P}(g) > C] \leq \delta.$$

*Proof:* See the Appendix. ■

The ability to provide a false positive guarantee for the constraint tests is a powerful yet natural consequence of the bound error rates. Indeed, we could not readily guarantee a false positive rate if using Monte Carlo estimates for the performance measures.

We noted in Section III that chance constraints:

$$\Pr[g \leq 0] \geq \tau$$

can be modeled using either a binary function for  $g \leq 0$  or by constraining  $\text{VaR}_\tau(g)$ . Using this equivalence, we can test whether a chance constraint holds via two equivalent methods:

- By forming  $\overline{\text{VaR}}_\tau = g_{(k)}$  using Theorem 1 and checking whether  $g_{(k)} \leq 0$ ,
- By first computing the number of successes/failures to satisfy  $g(\mathcal{X}, \mathcal{U}) \leq 0$  to form  $\bar{q}$  using Theorem 4 and checking whether  $\bar{q} \leq 1 - \tau$ .

Both methods also require the same number of minimum samples  $n$  to ever accept:  $\text{Bin}(n - 1; n, \tau) \geq 1 - \delta$ , although this condition is enforced directly in Theorem 1.

## V. BOUND EVALUATION EXPERIMENTS

In Fig. 3 we empirically validate the bounds given by Theorems 1, 2, 3, 4 (subfigures 3a, 3b, 3c, 3d respectively). We use the error rate  $\delta = 0.2$  for all bounds, and the quantile  $\tau = 0.7$  for  $\text{VaR}_\tau$  and  $\text{CVaR}_\tau$ . For a fixed open-loop policy  $\mathcal{U}$ , each plot shows the resulting distribution of total cost, as well as the distribution of the computed bound given  $n = 100$  samples. The blue dashed vertical line shows the true performance metric,<sup>2</sup> while the gray dashed vertical line shows the allowable error rate for the bound (0.2 in this case). The theorems state that the gray line lies to the right of the blue line, as shown in all the figures.

To emphasize that the bounds are agnostic to the form of the dynamics, we use a variety of MuJoCo environments for testing the validity of Theorems 1, 2, 3, 4 (Half Cheetah [52],

<sup>2</sup>Since we do not have access to the true underlying performance metric, we approximate the true metric with a Monte Carlo estimate from 10,000 simulation rollouts. This is only for visualization purposes.

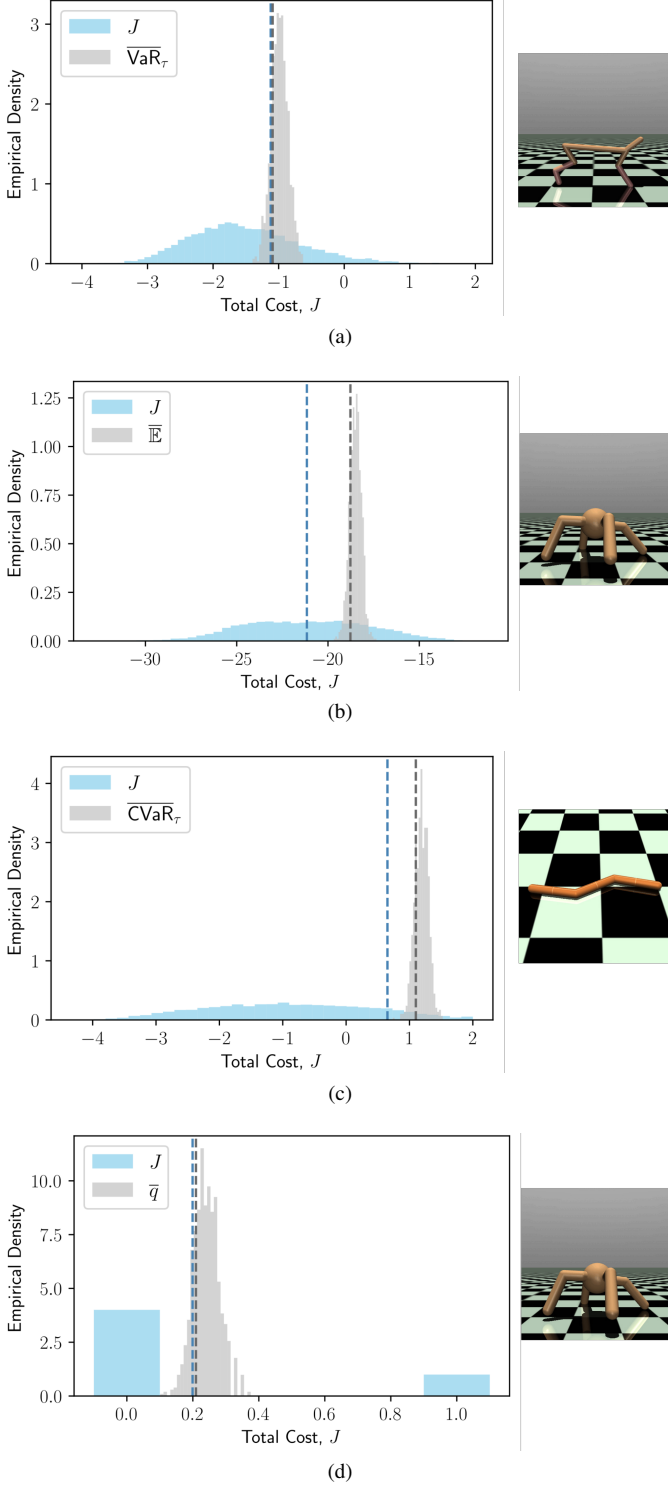


Figure 3. Empirical validation of the bounds for  $\text{VaR}_\tau$ ,  $\mathbb{E}$ ,  $\text{CVaR}_\tau$ , and  $q$  (subfigures 3a, 3b, 3c, 3d respectively). Each plot shows, for a single open-loop policy, the empirical distribution of total cost  $J$  (in blue), along with the distribution of the bound (in gray). The blue vertical line shows the true location of the measure we seek to bound ( $\text{VaR}_\tau(J)$ ,  $\mathbb{E}[J]$ ,  $\text{CVaR}_\tau(J)$ ,  $q$ , respectively) and the gray vertical line shows the  $\delta$  quantile of the associated bound. Our theoretical results ensure the gray line is to the right of the blue line, as validated in each plot. In each case  $n = 100$ ,  $\delta = 0.2$ , and for  $\text{VaR}_\tau$  and  $\text{CVaR}_\tau$ ,  $\tau = 0.7$ . Each histogram was generated using 10,000 simulations. To demonstrate that the bounds are agnostic to the dynamics, we used the Half Cheetah (3a), Ant (3b, 3d), and Swimmer (3c) MuJoCo environments.

Ant [53], Swimmer [54], and Ant again respectively). Due to limitations of the MuJoCo simulator, in these experiments, the dynamics of the robot are deterministic. Uncertainty comes from the starting state of the robot, which is randomly initialized using a Gaussian distribution centered about a nominal state. This form of uncertainty could realistically arise when a state estimation algorithm (e.g., Kalman filter) is used to provide a distribution over the starting state. The cost functions used are the negative values of the default rewards in MuJoCo, which encourage forward motion and minimal control input. We use clipping of the stage cost to ensure bounded support when computing the expectation and CVaR bounds. For the sparse cost case in subfigure 3d, we declared success, setting  $J = 0$ , when the Ant torso remained within the standard height range considered by default in MuJoCo, but still used the continuous cost when optimizing. The open-loop policies considered are obtained as the result of optimizing with the cross-entropy method (CEM) [55]. Thus, the bounds can be viewed as a formal guarantee on the optimizer’s solution performance under randomized initial conditions. Further experiment details are in the Appendix.

While the expectation and CVaR bound (Theorems 2, 3) are somewhat loose when using the relatively small number of 100 samples, the VaR and probability of failure bounds (Theorems 1, 4) are quite tight. In our later experiments, we focus on showing results using VaR as the relevant statistic.

In Fig. 4, using our approach from Theorem 5, we show the relationship between probability of our constraint test holding and the probability that the underlying constraint is actually satisfied. To convey the effect of sample size on the test we show theoretical curves for  $n \in \{10, 50, 100, 500\}$ . We empirically validate the theory for the  $n = 10$  case using simulations of the MuJoCo Ant environment. Specifically, the constraint function  $g = 0$  is a success if the height of the ant torso remains in the interval  $[0.5, 1]$  for an entire rollout (based on the healthy condition specified in MuJoCo), and a failure otherwise. We impose a binary failure probability constraint (10d) requiring that this condition is satisfied with probability at least  $\tau = 0.7$  (shown by the gray dotted vertical line in Fig. 4). In other words, we have reformulated a chance constraint as a constraint on the failure probability of a binary  $g$ . We seek to verify whether or not the provided control policy satisfies this constraint by using the test derived from Theorem 4, checking whether the upper bound on the failure probability is sufficiently low  $\bar{q} \leq 1 - \tau$ . By constructing  $\bar{q}$  with user-specified error rate of  $\delta = 0.2$  we are guaranteed to have a false positive error rate no greater than  $\delta = 0.2$  (shown by the dashed gray horizontal line in Fig. 4). To validate the test over a range of satisfying and violating policies, we use 20 open-loop policies generated by randomly sampling control actions.

For each policy, we repeatedly (1000 times) collect a fresh set of  $n = 10$  samples of the constraint function  $g_{1:n}$  by executing the control actions from random initial conditions in the Ant environment, and apply Theorem 5 with cutoff  $C = 1 - \tau$  and bound  $\bar{P} = \bar{q}$  computed from Theorem 4. We call each such bound computation a trial. We use the empirical fraction of trials for which we concluded the chance constraint



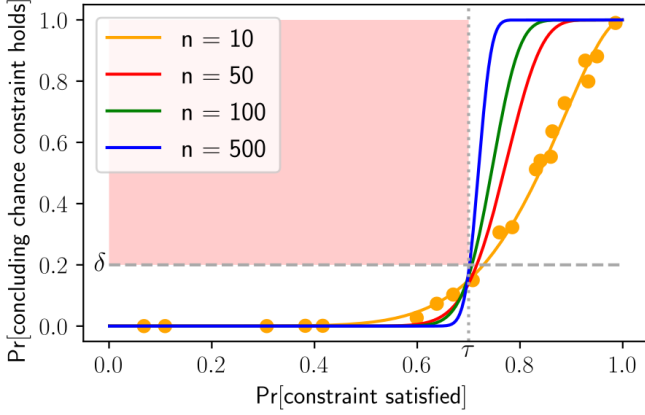


Figure 4. Visualization of Theorem 5, and empirical validation of the theorem, applied to testing whether a chance constraint holds. Each curve represents the probability of accepting that the chance constraint holds (y-axis) given the true probability of the underlying trajectory constraint being satisfied (x-axis). The validity of the theorem is demonstrated by each curve being below  $\delta$  when the chance constraint fails to hold i.e.,  $\text{Pr}[\text{constraint satisfied}]$  is below  $\tau$ . Visually, the false acceptance is guaranteed to be below  $\delta$  so that the curves avoid the region shaded in red in the figure. Here we use  $\delta = 0.2$  (horizontal line),  $\tau = 0.7$  (vertical line). Furthermore, as the sample size ( $n$ ) increases, the curve approaches a step function, i.e. we obtain a perfect discriminator. In addition, for  $n = 10$  we plot empirical results from the Ant environment where the vertical position of the Ant torso always being between  $[0.5, 1]$  with probability 0.7 is the chance constraint we seek to assess. The  $x$  and  $y$  coordinates for each orange dot are separately estimated using an average taken over 1000 simulation runs.

holds (based on the test) to approximate the unknown true probability. This fraction provides the y-coordinate for the associated point in the figure. We obtain the associated x-coordinate, the “ground truth” constraint satisfaction probability  $\text{Pr}[g = 0]$ , through 1000 Monte Carlo simulations. Specifically, we simulated the policy 1000 times and recorded the empirical fraction of the resulting trajectories that were a success, obtaining  $g = 0$ .

The tight agreement between the theoretical and empirical results show that we can use our method to provide a sampling-based certification method for policy constraint satisfaction. In particular, we observe that both in the empirical and theoretical curves whenever the constraint fails to hold, the acceptance probability is below  $\delta$ : to the left of the vertical line at  $\tau = 0.7$  all curves lie below the horizontal line at  $\delta = 0.2$ , avoiding the region shaded in red.

Similar figures could have been generated for constraint tests on other performance measures with continuous  $g$  e.g., a CVaR constraint. However, we would not easily be able to generate a corresponding theoretical curve. With Theorem 4, we can compute the theoretical curves using the Binomial distribution and the true probability of success.

## VI. POLICY SELECTION

Thus far we have presented a method for rigorously assessing the quality of a policy by placing bounds on performance measures of the trajectory cost and success. A natural extension is to use these bounds when selecting between several candidate policies. In this case, we must take care to apply an appropriate correction to the concentration bounds for the

resulting bound to remain probabilistically valid. To illustrate the need for a correction, consider a thought experiment where 100 identical policies are considered as candidates for execution. If there were no randomness in the bounds, all 100 policies would evaluate to the same performance bound. However, since the bounds hold probabilistically, one bound among the 100 is likely to be overly optimistic by chance, and may even be lower than the true VaR, i.e., an invalid bound. Choosing the lowest bound among the 100 will thus give an artificially low performance bound for the associated policy as the chosen bound is the result of a lucky draw of samples. To remedy this problem we explain a statistical correction for comparing bounds among a set of candidate policies.

### A. Coverage Correction

Consider  $m$  (not necessarily independent) policies  $\mathcal{U}_{1:m}$  where for each policy  $\mathcal{U}_i$  we obtain  $n$  IID trajectory rollouts, obtaining trajectory performance samples (cost or success) realizations  $S_{1:n}^{(i)}$ . Let the performance measure we are interested in be denoted by  $\mathcal{P}$  (e.g.  $\mathcal{P} = \text{VaR}_\tau$ ). Then, using the samples  $S_{1:n}^{(i)}$  and the results from Section IV, an individual upper bound  $\bar{P}^{(i)}$  is computed for each policy, which has corresponding unknown true performance  $P^{(i)}$ . Now suppose we plan to execute the policy with least upper bound, that is,

$$\mathcal{U}^* = \arg \min_{\mathcal{U}_i \in \mathcal{U}_{1:m}} \bar{P}^{(i)}. \quad (16)$$

Take  $\bar{P}^*$  as the individual upper bound associated with  $\mathcal{U}^*$  and  $P^*$  as the true statistic (e.g. true  $\text{VaR}_\tau$ ) associated with  $\mathcal{U}^*$ . We are interested in understanding with what probability  $\bar{P}^*$  upper bounds  $P^*$ , and formalize this in the below result.

**Theorem 6** (Uncorrected Coverage). *Suppose we are given  $m$  policies  $\mathcal{U}_{1:m}$ , with associated unknown true performance  $\{P^{(i)}\}_{i=1}^m$  and associated probabilistic bounds  $\{\bar{P}^{(i)}\}_{i=1}^m$  individually holding with coverage level  $1 - \delta$  i.e.,*

$$\text{Pr}[P^{(i)} \leq \bar{P}^{(i)}] \geq 1 - \delta \quad \forall i. \quad (17)$$

*Let  $\bar{P}^*$  be the lowest probabilistic bound and let  $P^*$  be the associated true statistic i.e.,*

$$i^* = \arg \min_{i \in \{1, \dots, m\}} \bar{P}^{(i)} \quad (18a)$$

$$\bar{P}^* = \bar{P}^{(i^*)} \quad (18b)$$

$$P^* = P^{(i^*)}. \quad (18c)$$

*Then,  $\bar{P}^*$  bounds  $P^*$  with probability at least  $(1 - \delta)^m$  i.e.,*

$$\text{Pr}[P^* \leq \bar{P}^*] \geq (1 - \delta)^m. \quad (19)$$

*Proof:* See the Appendix. ■

Before proceeding, we consider two limiting cases of Theorem 6. Temporarily assume that the bounds achieve the coverage level exactly i.e.,

$$\text{Pr}[P^{(i)} \leq \bar{P}^{(i)}] = 1 - \delta \quad (20)$$

then

- 1) When each bound is bounding the same statistic (i.e.,  $P^{(1)} = \dots = P^{(m)}$ ) then

$$\Pr[P^* \leq \bar{P}^*] = (1 - \delta)^m, \quad (21)$$

where this follows as all bounds must hold for the minimum bound to hold in this case.

- 2) When the support of the sample realizations associated with each  $\mathcal{U}_i$  is disjoint then

$$\Pr[P^* \leq \bar{P}^*] = 1 - \delta \quad (22)$$

where this follows as only one bound, the one with the lowest support interval, needs to hold for the minimum bound to hold in this case.

These two limiting cases show the extremes we must consider when making a coverage correction for multiple policies. In the best case (case 2), no loss of coverage is incurred, while in the worst case (case 1), the loss of coverage can be quite severe for a large set of candidates. Since we want to avoid distributional assumptions, we must consider the worst case scenario, in which case Theorem 6 is tight.

Theorem 6 captures the worst case coverage loss when comparing multiple policies and selecting the policy with lowest bound. Thus, we can use it to correct for the loss of coverage by first inflating the coverage level we require from each of the individual bounds produced for each policy, as described in the below Theorem.

**Theorem 7 (Coverage Correction).** *If a  $1 - \delta$  final level of coverage is desired when selecting among multiple policies, then the coverage level for each individual bound should be inflated to satisfy*

$$\Pr[P^{(i)} \leq \bar{P}^{(i)}] \geq 1 - \bar{\delta} \quad (23a)$$

$$\bar{\delta} = 1 - (1 - \delta)^{1/m}. \quad (23b)$$

**Remark (Multi-Hypothesis Connection).** *This correction is identical to the Šidák correction [56] for testing multiple hypotheses. Although we are only interested in ensuring that the minimizing bound be probabilistically valid, we end up needing to inflate as if we required all bounds to hold due to case 1 (the typical use case of multi-hypothesis correction).*

### B. Connection to Generalization in Machine Learning

Intuitively, this correction can also be understood from the perspective of machine learning generalization theory. In this analogy, we view choosing the policy as a model fitting problem. We evaluate one choice of model parameters, that is a policy  $\mathcal{U}_i$ , by computing a training loss  $\bar{P}^{(i)}$  using the simulated results  $S_{1:n}^{(i)}$ . However, there is discrepancy between the observed training performance and the true/expected test performance. Thus, when selecting the parameters  $\mathcal{U}^*$  which give best training performance it is important to account for this generalization gap, through the multi-hypothesis correction. This intuition can also help understand why a correction is still needed even if a fixed set of environments or uncertainty seeds were shared for evaluating all policies  $\mathcal{U}_{1:m}$ ; the potential for over-fitting to the training environments/seeds remains.

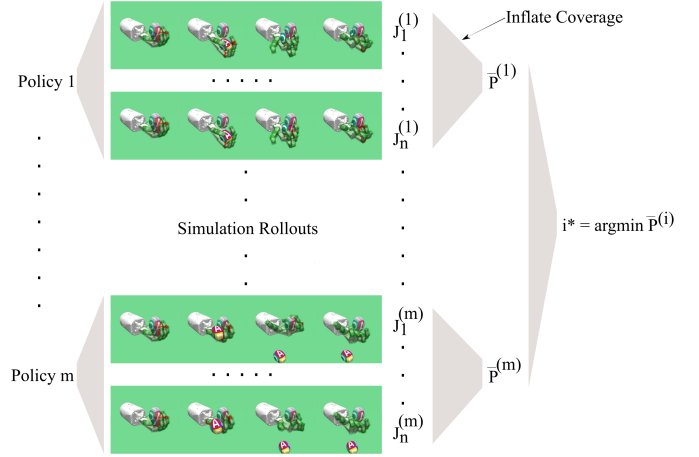


Figure 5. Overview of our method for comparing performance among a set of policies for manipulating an egg object of uncertain mass and friction with the MuJoCo Shadow Hand. Given  $m$  candidate policies, each policy is executed in simulation  $n$  times and the associated trajectory cost of each execution is recorded. These cost samples are then used to compute a probabilistic upper bound on performance for each policy  $\bar{P}^{(i)}$ . Lastly, the policy achieving the minimum bound is selected, giving a probabilistic guarantee on policy performance. To ensure that this final bound holds with a user-specified probability  $(1 - \delta)$ , we apply a multi-hypothesis correction to each of the individual bounds.

As mentioned previously, introducing the necessity of this bound correction is one of the main contributions of this paper. In Fig. 5 we summarize the process for selecting the policy with the lowest performance bound while retaining statistical validity using the multi-hypothesis correction. In Section VII we show the necessity of the correction by comparing against the naive uncorrected bound in the setting of object manipulation.

## VII. MANIPULATION EXAMPLE

In this section we demonstrate the validity and necessity of the multi-hypothesis correction in the MuJoCo Shadow Dexterous Hand environment [57] for simulating in-hand manipulation. In realistic settings, the object to be manipulated may have uncertain physical parameters such as mass and friction that can only be roughly estimated or inferred from interaction but are not directly observable. In this example, we show how for such a setting we can use our distribution-free method to select among several candidate control policies for manipulating the object, obtaining an associated performance bound for the chosen policy. This experiment is chosen to emphasize that our approach works with complex dynamics involving contact and the discontinuities therein.

To generate candidate policies, we use a simple sampling-based planner inspired by the approach in [58]. Critical to the success of the planner is not to sample actions for each step of the planning horizon, but to sub-sample a few “knot” points and fill in the remaining steps with a cubic spline interpolation. This has the effect of reducing the dimension of the action space as well as enforcing smoothness of the commanded joint positions. Using this method, we generated  $m = 20$  open-loop plans over a horizon of 100 timesteps each designed for manipulating Gymnasium’s egg object assuming a nominal

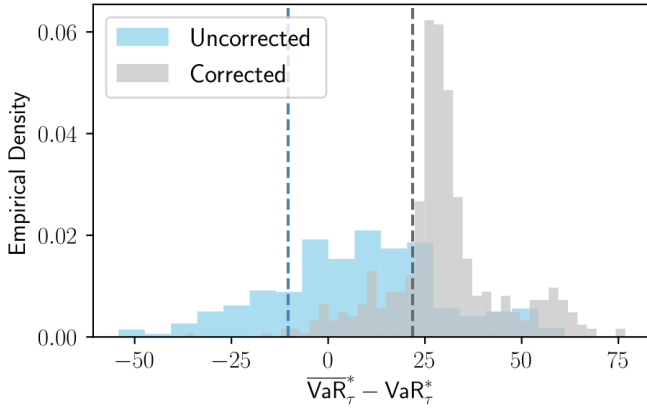


Figure 6. This figure shows the validity of the correction given by Theorem 7 for the Shadow Hand environment when manipulating the egg object with uncertain density and friction. Plotted are two distributions, of  $\text{VaR}_\tau^* - \text{VaR}_\tau$ . In blue  $\text{VaR}_\tau^*$  is chosen without the correction and in gray  $\text{VaR}_\tau^*$  is chosen with the multi-hypothesis correction specified in Theorem 7. Each sample in the histogram is generated by selecting the best among 20 pre-computed open-loop policies based on either the multi-hypothesis corrected or uncorrected bound. Each histogram is generated with 500 repetitions. Only for the corrected bound does the  $\delta$  quantile dashed line lie above 0. Thus, it is clear that when selecting a policy with multi-hypothesis correction the desired error rate is achieved, while this is not the case when using the uncorrected bound.

density of  $1000 \frac{\text{kg}}{\text{m}^3}$ , sliding friction coefficient of 1, torsional friction coefficient of 0.005, and rolling friction coefficient of 0.0001. We randomize over density rather than mass as this is more standard in MuJoCo, and the object volume is fixed, meaning that randomizing over density and mass are equivalent in this setting.

Given these candidate policies, we applied Theorem 7 to inflate coverage and select the bound-minimizing policy. We used  $\text{VaR}_\tau$  with  $\tau = 0.7$  as the cost performance measure we wish to bound and specified a bound error rate of  $\delta = 0.2$ . The policies are evaluated in simulated environments now randomizing the friction and density of the egg object to simulate uncertainty in the true object’s physical parameters. The specific uncertainties are

- density  $\sim \text{Uniform}[700, 1200] \frac{\text{kg}}{\text{m}^3}$
- sliding friction coefficient  $\sim \text{Uniform}[0.8, 1.2]$
- torsional friction coefficient  $\sim \text{Uniform}[0.004, 0.006]$
- rolling friction coefficient  $\sim \text{Uniform}[0.00008, 0.00014]$ .

The individual bound for each policy is computed using the total cost obtained in 30 simulated executions of it. The cost is based on aligning the egg with a desired goal position and orientation. The chosen goal orientation requires flipping the egg object from its starting orientation. Fig. 5 provides an overview of the policy selection and bound computation procedure used in this example and shows selected frames from simulations of the first and last of the 20 plans compared.

By repeatedly generating fresh cost samples to run many simulated experiments, we show in Fig. 6 that while our multi-hypothesis corrected bound is valid with at least the specified probability of  $1 - \delta$ , naively using the uncorrected bound is too optimistic and fails to achieve this coverage level.

## VIII. CONCLUSION

In this paper we demonstrated how sampling-based, distribution-free concentration bounds can be used to rigorously bound the performance of a control policy applied in a stochastic environment. These bounds can also be used to verify safety of a policy via constraint tests with a guaranteed false acceptance rate. We furthermore showed how to apply these bounds when selecting the best policy from a set of candidates which requires a multi-hypothesis correction to retain validity. Because these bounds are distribution-free, they can be applied to complex systems and uncertain environments without requiring knowledge of the underlying problem structure. Rather, our approach only requires simulating policy execution in the stochastic environment and recording the associated cost or constraint value. We empirically demonstrated bound validity in several MuJoCo environments including for the problem of object manipulation which is high-dimensional and has discontinuous dynamics.

In this work, we only studied a few performance measures but our approach extends to other measures if corresponding concentration bounds are available. We made the assumption that the simulative dynamics model exactly represents the dynamics encountered during execution. In practice this is never the case, and relaxing this assumption is important future work. Another interesting direction for future work is to use our method to select the best risk-sensitive plans in domain-randomized simulations that are then used as training data for a policy with hopes of better sim-to-real performance.

## ACKNOWLEDGMENTS

The authors would like to acknowledge Taylor Howell for his advisement on implementing the sampling based manipulation controller.

## REFERENCES

- [1] E. Todorov, T. Erez, and Y. Tassa, “Mujoco: A physics engine for model-based control,” in *2012 IEEE/RSJ international conference on intelligent robots and systems*, pp. 5026–5033, IEEE, 2012.
- [2] R. de Lazcano, K. Andreas, J. J. Tai, S. R. Lee, and J. Terry, “Gymnasium Robotics,” 2023.
- [3] P. Akella, M. Ahmadi, and A. D. Ames, “A scenario approach to risk-aware safety-critical system verification,” *arXiv preprint arXiv:2203.02595*, 2022.
- [4] H. Krasowski, P. Akella, A. Ames, and M. Althoff, “Verifiably Safe Reinforcement Learning with Probabilistic Guarantees via Temporal Logic,” *arXiv preprint arXiv:2212.06129*, 2022.
- [5] P. Akella, W. Ubellacker, and A. D. Ames, “Safety-Critical Controller Verification via Sim2Real Gap Quantification,” in *2023 IEEE International Conference on Robotics and Automation (ICRA)*, pp. 10539–10545, IEEE, 2023.
- [6] P. Akella, A. Dixit, M. Ahmadi, J. W. Burdick, and A. D. Ames, “Sample-based bounds for coherent risk measures: Applications to policy synthesis and verification,” *arXiv preprint arXiv:2204.09833*, 2022.

- [7] P. Akella, W. Ubellacker, and A. D. Ames, "Probabilistic Guarantees for Nonlinear Safety-Critical Optimal Control," *arXiv preprint arXiv:2303.06258*, 2023.
- [8] M. Cleaveland, L. Lindemann, R. Ivanov, and G. J. Pappas, "Risk verification of stochastic systems with neural network controllers," *Artificial Intelligence*, vol. 313, p. 103782, 2022.
- [9] A. Dvoretzky, J. Kiefer, and J. Wolfowitz, "Asymptotic minimax character of the sample distribution function and of the classical multinomial estimator," *The Annals of Mathematical Statistics*, pp. 642–669, 1956.
- [10] P. Massart, "The tight constant in the Dvoretzky-Kiefer-Wolfowitz inequality," *The annals of Probability*, pp. 1269–1283, 1990.
- [11] S. Carpin, Y.-L. Chow, and M. Pavone, "Risk aversion in finite Markov Decision Processes using total cost criteria and average value at risk," in *2016 IEEE international conference on robotics and automation (ICRA)*, pp. 335–342, IEEE, 2016.
- [12] M. Ahmadi, X. Xiong, and A. D. Ames, "Risk-averse control via CVaR barrier functions: Application to bipedal robot locomotion," *IEEE Control Systems Letters*, vol. 6, pp. 878–883, 2021.
- [13] T. Lew, R. Bonalli, and M. Pavone, "Chance-constrained sequential convex programming for robust trajectory optimization," in *2020 European Control Conference (ECC)*, pp. 1871–1878, IEEE, 2020.
- [14] A. Hakobyan and I. Yang, "Wasserstein distributionally robust motion control for collision avoidance using conditional value-at-risk," *IEEE Transactions on Robotics*, vol. 38, no. 2, pp. 939–957, 2021.
- [15] A. Navsalkar and A. R. Hota, "Data-Driven Risk-sensitive Model Predictive Control for Safe Navigation in Multi-Robot Systems," in *2023 IEEE International Conference on Robotics and Automation (ICRA)*, pp. 1442–1448, IEEE, 2023.
- [16] A. Dixit, M. Ahmadi, and J. W. Burdick, "Risk-sensitive motion planning using entropic value-at-risk," in *2021 European Control Conference (ECC)*, pp. 1726–1732, IEEE, 2021.
- [17] E. R. Hunt, C. B. Cullen, and S. Hauert, "Value at Risk strategies for robot swarms in hazardous environments," in *Unmanned Systems Technology XXIII*, vol. 11758, pp. 158–177, SPIE, 2021.
- [18] T. Hiraoka, T. Imagawa, T. Mori, T. Onishi, and Y. Tsuruoka, "Learning robust options by conditional value at risk optimization," *Advances in Neural Information Processing Systems*, vol. 32, 2019.
- [19] K. Chua, R. Calandra, R. McAllister, and S. Levine, "Deep reinforcement learning in a handful of trials using probabilistic dynamics models," *Advances in neural information processing systems*, vol. 31, 2018.
- [20] R. Dyro, J. Harrison, A. Sharma, and M. Pavone, "Particle MPC for Uncertain and Learning-Based Control," in *2021 IEEE/RSJ International Conference on Intelligent Robots and Systems (IROS)*, pp. 7127–7134, IEEE, 2021.
- [21] T. Lew, R. Bonalli, and M. Pavone, "Sample Average Approximation for Stochastic Programming with Equality Constraints," *arXiv preprint arXiv:2206.09963*, 2022.
- [22] T. Lew, R. Bonalli, and M. Pavone, "Risk-Averse Trajectory Optimization via Sample Average Approximation," *arXiv preprint arXiv:2307.03167*, 2023.
- [23] G. Shafer and V. Vovk, "A Tutorial on Conformal Prediction," *Journal of Machine Learning Research*, vol. 9, no. 3, 2008.
- [24] R. Luo, S. Zhao, J. Kuck, B. Ivanovic, S. Savarese, E. Schmerling, and M. Pavone, "Sample-efficient safety assurances using conformal prediction," in *International Workshop on the Algorithmic Foundations of Robotics*, pp. 149–169, Springer, 2023.
- [25] L. Lindemann, M. Cleaveland, G. Shim, and G. J. Pappas, "Safe planning in dynamic environments using conformal prediction," *IEEE Robotics and Automation Letters*, 2023.
- [26] A. Dixit, L. Lindemann, S. X. Wei, M. Cleaveland, G. J. Pappas, and J. W. Burdick, "Adaptive conformal prediction for motion planning among dynamic agents," in *Learning for Dynamics and Control Conference*, pp. 300–314, PMLR, 2023.
- [27] D. B. Brown, "Large deviations bounds for estimating conditional value-at-risk," *Operations Research Letters*, vol. 35, no. 6, pp. 722–730, 2007.
- [28] Y. Wang and F. Gao, "Deviation inequalities for an estimator of the conditional value-at-risk," *Operations Research Letters*, vol. 38, no. 3, pp. 236–239, 2010.
- [29] P. Thomas and E. Learned-Miller, "Concentration inequalities for conditional value at risk," in *International Conference on Machine Learning*, pp. 6225–6233, PMLR, 2019.
- [30] R. K. Kolla, L. Prashanth, S. P. Bhat, and K. Jagannathan, "Concentration bounds for empirical conditional value-at-risk: The unbounded case," *Operations Research Letters*, vol. 47, no. 1, pp. 16–20, 2019.
- [31] W. Hoeffding, "Probability Inequalities for Sums of Bounded Random Variables," *Journal of the American Statistical Association*, vol. 58, no. 301, pp. 13–30, 1963.
- [32] L. Prashanth and S. P. Bhat, "A Wasserstein distance approach for concentration of empirical risk estimates," *The Journal of Machine Learning Research*, vol. 23, no. 1, pp. 10830–10890, 2022.
- [33] B. Szorenyi, R. Busa-Fekete, P. Weng, and E. Hüllermeier, "Qualitative multi-armed bandits: A quantile-based approach," in *International Conference on Machine Learning*, pp. 1660–1668, PMLR, 2015.
- [34] S. R. Howard and A. Ramdas, "Sequential estimation of quantiles with applications to A/B testing and best-arm identification," *Bernoulli*, vol. 28, no. 3, pp. 1704–1728, 2022.
- [35] R. Zieliński and W. Zieliński, "Best exact nonparametric confidence intervals for quantiles," *Statistics*, vol. 39, no. 1, pp. 67–71, 2005.
- [36] H. Scheffe and J. W. Tukey, "Non-parametric estimation. I. Validation of order statistics," *The Annals of Mathematical Statistics*, vol. 16, no. 2, pp. 187–192, 1945.
- [37] H. A. David and H. N. Nagaraja, *Order statistics*. John Wiley & Sons, 2004.

- [38] T. W. Anderson, “Confidence limits for the expected value of an arbitrary bounded random variable with a continuous distribution function,” tech. rep., Stanford University Department of Statistics, 1969.
- [39] M. Phan, P. Thomas, and E. Learned-Miller, “Towards practical mean bounds for small samples,” in *International Conference on Machine Learning*, pp. 8567–8576, PMLR, 2021.
- [40] S. R. Howard, A. Ramdas, J. McAuliffe, and J. Sekhon, “Time-uniform, nonparametric, nonasymptotic confidence sequences,” *The Annals of Statistics*, vol. 49, no. 2, 2021.
- [41] L. D. Brown, T. T. Cai, and A. DasGupta, “Interval estimation for a binomial proportion,” *Statistical science*, vol. 16, no. 2, pp. 101–133, 2001.
- [42] A. M. Pires and C. Amado, “Interval estimators for a binomial proportion: Comparison of twenty methods,” *REVSTAT-Statistical Journal*, vol. 6, no. 2, pp. 165–197, 2008.
- [43] C. J. Clopper and E. S. Pearson, “The use of confidence or fiducial limits illustrated in the case of the binomial,” *Biometrika*, vol. 26, no. 4, pp. 404–413, 1934.
- [44] T. E. Sterne, “Some remarks on confidence or fiducial limits,” *Biometrika*, vol. 41, no. 1/2, pp. 275–278, 1954.
- [45] E. L. Crow, “Confidence intervals for a proportion,” *Biometrika*, vol. 43, no. 3/4, pp. 423–435, 1956.
- [46] M. W. Eudey, *I. On the Treatment of Discontinuous Random Variables. II. Statistical Model for Comparing Two Methods of Diagnosis*. PhD thesis, University of California - Berkeley, 1949.
- [47] E. L. Lehmann and J. P. Romano, *Testing statistical hypotheses*, vol. 4. Springer, 2022.
- [48] W. L. Stevens, “Fiducial limits of the parameter of a discontinuous distribution,” *Biometrika*, vol. 37, no. 1/2, pp. 117–129, 1950.
- [49] W. Wang, “Smallest confidence intervals for one binomial proportion,” *Journal of Statistical Planning and Inference*, vol. 136, no. 12, pp. 4293–4306, 2006.
- [50] V. Vovk, “Conditional validity of inductive conformal predictors,” in *Asian conference on machine learning*, pp. 475–490, PMLR, 2012.
- [51] A. N. Angelopoulos and S. Bates, “A gentle introduction to conformal prediction and distribution-free uncertainty quantification,” *arXiv preprint arXiv:2107.07511*, 2021.
- [52] P. Wawrzyński, “A cat-like robot real-time learning to run,” in *Adaptive and Natural Computing Algorithms: 9th International Conference, ICANNGA 2009, Kuopio, Finland, April 23-25, 2009, Revised Selected Papers 9*, pp. 380–390, Springer, 2009.
- [53] J. Schulman, P. Moritz, S. Levine, M. Jordan, and P. Abbeel, “High-dimensional continuous control using generalized advantage estimation,” *arXiv preprint arXiv:1506.02438*, 2015.
- [54] R. Coulom, *Reinforcement learning using neural networks, with applications to motor control*. PhD thesis, Institut National Polytechnique de Grenoble-INPG, 2002.
- [55] S. Mannor, R. Y. Rubinstein, and Y. Gat, “The cross entropy method for fast policy search,” in *Proceedings of the 20th International Conference on Machine Learning (ICML-03)*, pp. 512–519, 2003.
- [56] H. Abdi, “The Bonferonni and Šidák Corrections for Multiple Comparisons,” *Encyclopedia of measurement and statistics*, vol. 3, 01 2007.
- [57] A. Melnik, L. Lach, M. Plappert, T. Korthals, R. Haschke, and H. Ritter, “Using tactile sensing to improve the sample efficiency and performance of deep deterministic policy gradients for simulated in-hand manipulation tasks,” *Frontiers in Robotics and AI*, p. 57, 2021.
- [58] T. Howell, N. Gileadi, S. Tunyasuvunakool, K. Zakka, T. Erez, and Y. Tassa, “Predictive Sampling: Real-time Behaviour Synthesis with MuJoCo,” *arXiv preprint arXiv:2212.00541*, 2022.
- [59] A. Shapiro, D. Dentcheva, and A. Ruszczyński, *Lectures on stochastic programming: modeling and theory*. SIAM, 2021.
- [60] R. Hulsman, “Distribution-Free Finite-Sample Guarantees and Split Conformal Prediction,” *arXiv preprint arXiv:2210.14735*, 2022.

## APPENDIX

## A. Simulation Details for Figure 3

We perturbed the default starting state in MuJoCo using `reset_noise_scale = 0.1`. The sole exception to this was for the sparse cost case with the Ant where we used `reset_noise_scale = 0.3` since the default of 0.1 was never enough to push the Ant outside the healthy range of  $[0.2, 1]$  when using the action sequence optimized by CEM.

To identify the candidate policy, cross entropy method (CEM) [55] was used. 10 generations of optimization were performed, where in each generation 100 open-loop policies were generated by sampling the control input at each timestep using a Gaussian distribution based on the estimated mean and variance from the previous generation. Based on a single execution in the random environment, the top performing 10 sample plans were then used to fit the Gaussian distribution for the next generation. After the final generation, the top performing plan was selected as the candidate. Plans had a horizon of 20 timesteps.

To approximate the theoretical distribution over cost, the candidate policy was executed 1000 times. The associated theoretical statistic was then found separately by taking the empirical average cost for  $\mathbb{E}$ , the empirical quantile for  $\text{VaR}_\tau$ , or the Monte Carlo approximation for  $\text{CVaR}_\tau$  (see [59]). To compute  $\mathbb{E}$  and  $\text{CVaR}_\tau$ , the total costs in the Ant environment were clipped to between  $[-2H, 0]$  and between  $[-0.325H, 0.1H]$  for the Swimmer environment where  $H = 20$  was the horizon.

## B. Proof of Theorem 1

## 1) Upper Bound:

**Lemma 1.**

$$\Pr[J_i < \text{VaR}_\tau(J)] \leq \tau \quad (24)$$

*Proof:* We may rewrite the strict inequality probability using a left limit approaching  $\text{VaR}_\tau(J)$ :

$$\Pr[J_i < \text{VaR}_\tau(J)] = \lim_{x \rightarrow \text{VaR}_\tau(J)^-} \Pr[J_i \leq x] \quad (25)$$

and are guaranteed that the limit exists since CDFs are upper semicontinuous. Since  $x$  in the limit satisfies  $x < \text{VaR}_\tau(J)$ , by definition of  $\text{VaR}$  as an infimum we have

$$\Pr[J_i \leq x] < \tau. \quad (26)$$

Since this holds for all  $x$  in the limit,

$$\lim_{x \rightarrow \text{VaR}_\tau(J)^-} \Pr[J_i \leq x] \leq \tau \quad (27)$$

concluding the proof.  $\blacksquare$

Using the definition of  $\text{VaR}_\tau(J)$  we have

$$\Pr[\text{VaR}_\tau(J) \leq J_{(k)}] = \Pr\left[\sum_{i=1}^n \mathbb{1}(J_i < \text{VaR}_\tau(J)) < k\right] \quad (28a)$$

$$= \Pr\left[\sum_{i=1}^n \mathbb{1}(J_i < \text{VaR}_\tau(J)) \leq k - 1\right]. \quad (28b)$$

Since by Lemma 1 we have

$$\Pr[J_i < \text{VaR}_\tau(J)] \leq \tau, \quad (29)$$

the random quantity  $\mathbb{1}(J_i < \text{VaR}_\tau(J))$  is Bernoulli where the probability of being 1 is at most  $\tau$ . Thus,

$$\Pr\left[\sum_{i=1}^n \mathbb{1}(J_i < \text{VaR}_\tau(J)) \leq k - 1\right] \geq \text{Bin}(k - 1; n, \tau) \quad (30)$$

since we have the sum of  $n$  IID Bernoulli random variables with probability of being 1 at most  $\tau$ .

Therefore, given values for  $\tau, \delta \in (0, 1)$  and  $J_{1:n}$ , choosing

$$\overline{\text{VaR}}_\tau = J_{(k)} \quad (31a)$$

$$k = \min\{k' \mid \text{Bin}(k' - 1; n, \tau) \geq 1 - \delta\} \quad (31b)$$

ensures that

$$\Pr[\text{VaR}_\tau(J) \leq \overline{\text{VaR}}_\tau] \geq 1 - \delta. \quad (32)$$

$\blacksquare$

**Remark.** Note that in the case where  $J$  has invertible CDF, (29) is tight so that (30) holds exactly. In fact, we can then give a more precise result in this case,

$$1 - \delta \leq \Pr[\text{VaR}_\tau(J) \leq \overline{\text{VaR}}_\tau] \leq 1 - \delta + \text{bin}(k - 1; n, \tau) \quad (33)$$

where  $k$  is the order statistic chosen for  $\overline{\text{VaR}}_\tau$  and  $\text{bin}(k - 1; n, \tau)$  denotes the Binomial probability mass function evaluated at  $k - 1$  successes. Thus, the amount of conservatism in the coverage is no more than  $\text{bin}(k - 1; n, \tau)$ .

**Remark.** Alternatively, we may also achieve exactly the desired coverage by randomizing which order statistic we choose, randomly selecting between the  $k$  which just undercovers and the one which just overcovers, weighting the selection probabilities to perfectly meet  $1 - \delta$  (see [35] for more details).

**Remark.** In deriving the bound for  $\text{VaR}$ , we were able to adapt a very similar conditional result from conformal prediction presented below (see [60] for more details).

**Theorem 8** (Conformal Prediction Conditional Result). *Given  $n + 1$  IID samples  $S_{1:n+1}$  from some continuous distribution  $S \sim \mathcal{D}$ ,*

$$\Pr\left[\Pr[S_{n+1} \leq S_{(k)} \mid S_{1:n}] \geq 1 - \epsilon\right] = \text{Bin}(k - 1; n, 1 - \epsilon). \quad (34)$$

*In fact, our proof does not assume a continuous distribution  $\mathcal{D}$  and can be applied to adapt the above result to  $\geq \text{Bin}(k - 1; n, 1 - \epsilon)$  for any distribution.*

2) *2-Sided Bound:* Assume  $J$  has invertible CDF. For  $1 \leq l < u \leq n$  we have

$$\begin{aligned} \Pr[J_{(l)} \leq \text{VaR}_\tau(J) \leq J_{(u)}] \\ = \Pr\left[l < \sum_{i=1}^n \mathbb{1}(J_i < \text{VaR}_\tau(J)) < u\right] \end{aligned} \quad (35a)$$

$$= \Pr[l + 1 \leq \sum_{i=1}^n \mathbb{1}(J_i < \text{VaR}_\tau(J)) \leq u - 1] \quad (35b)$$

$$= \text{Bin}(u - 1; n, \tau) - \text{Bin}(l + 1; n, \tau). \quad (35c)$$



where for the last equality we have used a general property of CDFs.

Then, given values for  $\tau, \delta \in (0, 1)$  and  $J_{1:n}$ , choosing  $l, u$  such that

$$\text{Bin}(u-1; n, \tau) - \text{Bin}(l+1; n, \tau) \geq 1 - \delta \quad (36)$$

ensures the desired bound holds.

Feasible values for  $l, u$  exist when  $n$  is large enough to ensure

$$\text{Bin}(n-1; n, \tau) - \text{Bin}(2; n, \tau) \geq 1 - \delta. \quad (37)$$

■

### C. Proof of Theorem 2

1) *Upper Bound*: The result follows as a special case of Theorem 3 proven below. We let  $\tau = 0$ , noting that  $\overline{\text{CVaR}}_\tau = \mathbb{E}$  when  $\tau = 0$  from the definitions of  $\text{CVaR}_\tau$  and  $\mathbb{E}$  in Def. 3 and Def. 2, respectively.

■

2) *2-Sided Bound*: Similarly, the 2-sided bound is obtained from the 2-sided  $\text{CVaR}_\tau$  bound in the proof of Theorem 3 below by setting  $\tau = 0$ . We obtain the lower bound

$$\mathbb{E} = \epsilon y_{\text{lb}} + \left(1 - \frac{k_u - 1}{n} - \epsilon\right) Y_{(k_u)} + \frac{1}{n} \sum_{i=1}^{k_u-1} Y_{(i)},$$

which holds with probability  $1 - \delta$ . Applying the bounds simultaneously using the inclusion-exclusion principle as in the  $\text{CVaR}$  case gives

$$\Pr[\mathbb{E} \leq \mathbb{E}[Y] \leq \mathbb{E}] \geq (1 - 2\delta).$$

■

### D. Proof of Theorem 3

1) *Upper Bound*: To construct an upper bound for  $\text{CVaR}$  we first revisit the definition,

$$\text{CVaR}_\tau(Y) := \frac{1}{1-\tau} \int_\tau^1 \text{VaR}_\gamma(Y) d\gamma. \quad (38)$$

Note that if we can construct an upper bound on the  $\text{VaR}$  that holds for all  $\gamma$ , then we can use this to find an upper bound on the  $\text{CVaR}$ ,

$$\overline{\text{CVaR}}_\tau(Y) = \frac{1}{1-\tau} \int_\tau^1 \overline{\text{VaR}}_\gamma(Y) d\gamma. \quad (39)$$

Note the slight abuse of notation here, in this proof we require a *simultaneous*  $\text{VaR}$  bound for which

$$\Pr[\overline{\text{VaR}}_\tau \geq \text{VaR}_\tau \quad \forall \tau] \geq 1 - \delta, \quad (40)$$

a stronger requirement than we had for the  $\text{VaR}$  bound presented in Theorem 1. Next we describe how we obtain a simultaneous  $\text{VaR}$  bound.

Consider IID samples  $Y_1, \dots, Y_n$  with unknown distribution  $\text{CDF}(y)$  and let  $y_{\text{ub}}$  be an associated almost sure upper bound.<sup>3</sup> Let  $\widehat{\text{CDF}}(y)$  be the empirical CDF,

$$\widehat{\text{CDF}}(y) = \frac{1}{n} \sum_{i=1}^n \mathbb{1}(Y_i \leq y), \quad (41)$$

and  $\epsilon(n, \delta)$  is a constant subtracted from  $\widehat{\text{CDF}}(y)$  to obtain a probabilistic lower bound  $\underline{\text{CDF}}(y) = \max\{\widehat{\text{CDF}}(y) - \epsilon, 0\}$  for  $y < y_{\text{ub}}$  and  $\underline{\text{CDF}}(y) = 1$  for  $y \geq y_{\text{ub}}$ . By letting

$$\epsilon(n, \delta) = \sqrt{\frac{-\ln(\delta)}{2n}}, \quad (42)$$

(what we call the DKW gap in Def. 7) we know from the DKW bound [9, 10] that

$$\Pr[\underline{\text{CDF}}(y) \leq \text{CDF}(y) \quad \forall y] \geq 1 - \delta. \quad (43)$$

Let  $\overline{\text{VaR}}_\tau$  be the  $\text{VaR}_\tau$  obtained from  $\underline{\text{CDF}}(y)$ , and note that the DKW bound extends to  $\overline{\text{VaR}}_\tau$  to give

$$\Pr[\overline{\text{VaR}}_\tau \geq \text{VaR}_\tau \quad \forall \tau] \geq 1 - \delta. \quad (44)$$

To see this, observe that  $\underline{\text{CDF}}(y) \leq \text{CDF}(y)$  for all  $y$  implies  $\{y \mid \underline{\text{CDF}}(y) \geq \tau\} \subseteq \{y \mid \text{CDF}(y) \geq \tau\}$ , therefore  $\inf\{y \mid \underline{\text{CDF}}(y) \geq \tau\} \geq \inf\{y \mid \text{CDF}(y) \geq \tau\}$ , since the inf over a subset is greater than or equal to the inf over the larger set. We have  $\underline{\text{CDF}}(y) \leq \text{CDF}(y)$  for all  $y$  implies  $\overline{\text{VaR}}_\tau \geq \text{VaR}_\tau$  for all  $\tau$  (from the definition of  $\text{VaR}_\tau$  in Def. 1). The extension of the DKW bound to  $\overline{\text{VaR}}_\tau$  follows.

From this bound, we conclude that integrating  $\overline{\text{VaR}}_\tau$  over any  $\tau$  interval gives an upper bound on the integral of  $\text{VaR}_\tau$  over the same interval, which holds with probability at least  $1 - \delta$ . We proceed to analytically integrate  $\overline{\text{VaR}}_\tau$  from  $\tau$  to 1 to compute  $\overline{\text{CVaR}}_\tau$  based on the definition of  $\text{CVaR}_\tau$  in Def. 3.

Note that  $\overline{\text{VaR}}_\tau$  is a staircase function defined on the domain  $\tau \in [0, 1]$ , which is equal to the smallest order statistic  $Y_{(k)}$  such that  $(\frac{k}{n} - \epsilon) \geq 0$  over the interval  $\tau \in [0, (\frac{k}{n} - \epsilon)]$ . It is then equal to  $Y_{(k+1)}$  over the next interval  $\tau \in ((\frac{k}{n} - \epsilon), (\frac{k+1}{n} - \epsilon)]$ , proceeding to  $Y_{(n)}$  over  $\tau \in ((\frac{n-1}{n} - \epsilon), (1 - \epsilon)]$ , and finally  $y_{\text{ub}}$  over the last interval of  $\tau \in ((1 - \epsilon), 1]$ . Notice that all intervals are of length  $\frac{1}{n}$ , except for the first, which is of length  $(\frac{k}{n} - \epsilon)$ , and the last, which is of length  $\epsilon$ .

Integrating this staircase function from a given  $\tau$  to 1, therefore, evaluates to a sum over order statistics times the length of their respective intervals. The first order statistic in this sum is the smallest such that its interval appears above the  $\tau$  quantile, namely  $Y_{(k)}$ , where  $k$  is the smallest index such that  $(\frac{k}{n} - \epsilon) \geq \tau$ . The length of this first interval is then  $(\frac{k}{n} - \epsilon - \tau)$ , and we have for the first term in the sum  $(\frac{k}{n} - \epsilon - \tau)Y_{(k)}$ , followed by  $n - k$  terms of the form  $\frac{1}{n}Y_{(i)}$ , where  $i = k + 1, \dots, n$ , and finally the term  $\epsilon y_{\text{ub}}$ . Following the definition of  $\text{CVaR}_\tau$  in Def. 3, we normalize the sum by the length of the interval over which we integrate,  $\frac{1}{1-\tau}$ , to obtain the desired expression.

The bound holds for any  $\tau \in [0, 1)$  and  $\delta \in (0, 0.5]$  (this requirement comes from the DKW inequality). To avoid

<sup>3</sup>We replace our  $J$  notation with  $Y$  to avoid potential confusion of  $j$  as an index.

defaulting to  $y_{ub}$  we require that there is an index  $k \leq n$  such that  $(\frac{k}{n} - \epsilon - \tau) \geq 0$ . Equivalently,  $\epsilon \leq 1 - \tau$  which implies  $n \geq -\frac{1}{2} \ln(\delta)/(1 - \tau)^2$ .

As noted earlier, this CVaR bound is mathematically equivalent to the one in [29], but our derivation results in a different form for the bound expression. Visualizations of the integral form of CVaR are given in Figures 3 and 4 of [29].

■

2) *2-Sided Bound*: To produce a 2-sided bound, we first prove a 1-sided lower CVaR bound, then combine the two bounds to get a 2-sided bound. For the CVaR lower bound we require knowledge of an *a priori* almost sure lower bound on  $Y$ , symmetrically with the almost sure upper bound  $y_{ub}$  required for the probabilistic CVaR upper bound. To streamline notation, we define  $Y_{(0)} = y_{lb}$ .

We use the same approach as in the CVaR upper bound, but we invoke the DKW upper-bound (instead of the lower-bound used before)

$$\Pr[\text{CDF}(y) \leq \overline{\text{CDF}}(y) \forall y] \geq 1 - \delta, \quad (45)$$

where  $\overline{\text{CDF}}(y)$  is the probabilistic upper bound on the CDF by shifting the empirical CDF upward by  $\epsilon$ , capping at 1 above, and using a lower bound to cap the support over  $y$  from below. Specifically, we define  $\overline{\text{CDF}}(y) = \min\{\overline{\text{CDF}}(y) + \epsilon, 1\}$  for  $y \geq y_{lb}$  and  $\overline{\text{CDF}}(y) = 0$  for  $y < y_{lb}$ . Define  $\text{VaR}_\tau$  as the  $\text{VaR}_\tau$  obtained from  $\overline{\text{CDF}}(y)$ , and extend the DKW upper bound to give a  $\text{VaR}_\tau$  lower bound,

$$\Pr[\text{VaR}_\tau \leq \text{VaR}_\tau \forall \tau] \geq 1 - \delta. \quad (46)$$

Integrating  $\text{VaR}_\tau$  analytically from  $\tau$  to 1 and normalizing by  $(1 - \tau)$  gives

$$\begin{aligned} \text{CVaR}_\tau = \frac{1}{1 - \tau} & \left[ \left( \frac{k_l}{n} + \epsilon - \tau \right) Y_{(k_l)} + \right. \\ & \left. \left( 1 - \frac{k_u - 1}{n} - \epsilon \right) Y_{(k_u)} + \frac{1}{n} \sum_{i=k_l+1}^{k_u-1} Y_{(i)} \right], \end{aligned} \quad (47)$$

where  $k_l \in \{0, 1, \dots, n\}$  is the smallest index (including 0) such that  $(\frac{k_l}{n} + \epsilon - \tau) \geq 0$ , defining the first stair step appearing in the integral, and  $k_u$  is the largest index such that  $(1 - \frac{k_u - 1}{n} - \epsilon) > 0$ , defining the last stair step appearing in the integral. If  $k_l + 1 = k_u$ , we ignore the sum. If  $k_l = k_u$  then we must modify the bound to have the right length of  $(1 - \tau)$  associated with the single step  $Y_{(k_u)}$  included in the integral, yielding

$$\text{CVaR}_\tau = Y_{(k_u)} \quad (48)$$

This bound applies for  $\tau \in [0, 1)$  and  $\delta \in (0, 0.5]$ , and we require the number of samples  $n \geq -\frac{1}{2} \ln(\delta)$ , to ensure  $\epsilon \leq 1$ .

Then given that the upper and lower bounds hold individually with probability  $1 - \delta$ , we can use the inclusion-exclusion principle to show that the bounds hold simultaneously with

probability  $1 - 2\delta$ . We have

$$\begin{aligned} & \mathbb{P}[\text{CVaR}_\tau \leq \text{CVaR}_\tau \leq \overline{\text{CVaR}}_\tau] \\ &= \mathbb{P}[\text{CVaR}_\tau \leq \text{CVaR}_\tau] + \mathbb{P}[\text{CVaR}_\tau \leq \overline{\text{CVaR}}_\tau] \end{aligned} \quad (49a)$$

$$\begin{aligned} & - \mathbb{P}[\text{CVaR}_\tau \leq \text{CVaR}_\tau \cup \text{CVaR}_\tau \leq \overline{\text{CVaR}}_\tau] \\ & \geq (1 - \delta) + (1 - \delta) \end{aligned} \quad (49b)$$

$$\begin{aligned} & - (1 - \mathbb{P}[\text{CVaR}_\tau > \text{CVaR}_\tau \cap \text{CVaR}_\tau > \overline{\text{CVaR}}_\tau]) \\ & = 2(1 - \delta) - (1 - 0) = 1 - 2\delta. \end{aligned} \quad (49c)$$

where we have used that  $\text{CVaR}_\tau \leq \overline{\text{CVaR}}_\tau$  to conclude that

$$\begin{aligned} & \mathbb{P}[\text{CVaR}_\tau > \text{CVaR}_\tau \cap \text{CVaR}_\tau > \overline{\text{CVaR}}_\tau] \\ &= \mathbb{P}[\text{CVaR}_\tau > \text{CVaR}_\tau > \overline{\text{CVaR}}_\tau] \end{aligned} \quad (50a)$$

$$\leq \mathbb{P}[\text{CVaR}_\tau > \overline{\text{CVaR}}_\tau] = 0. \quad (50b)$$

■

#### E. Proof of Theorem 4

Let  $J = 0$  denote success and  $J = 1$  failure for a Bernoulli random variable. Our goal is to produce an upper bound for the probability of failure  $q = \Pr[J = 1]$  which is unknown. We will do so by first obtaining a lower bound on the probability of success  $p = \Pr[J = 0] = 1 - q$  i.e., find  $\tau$  such that  $\Pr[J = 0] \geq \tau$ .

We can reformulate this in terms of the VaR of  $J$ ,

$$\Pr[J = 0] = \Pr[J \leq 0] \geq \tau \iff \text{VaR}_\tau(J) \leq 0. \quad (51)$$

Thus, to find the tightest lower bound, denoted  $\tau^*$  we can equivalently find the largest  $\tau$  such that  $\text{VaR}_\tau(J) \leq 0$ . However, we do not know  $\text{VaR}_\tau(J)$ . Thus, we instead leverage our earlier, sampling-based bound on the VaR. Given  $n$  IID samples  $J_{1:n}$ , we can compute  $\overline{\text{VaR}}_\tau$  using Theorem 1 and consider  $\tau$  for which  $\overline{\text{VaR}}_\tau \leq 0$ .

In other words, we arrive at the optimization

$$\tau^* = \max\{\tau \in [0, 1] \mid \overline{\text{VaR}}_\tau \leq 0\}. \quad (52)$$

From Theorem 1,

$$\overline{\text{VaR}}_\tau = J_{(k)} \quad (53a)$$

$$k = \min\{k' \mid \text{Bin}(k' - 1; n, \tau) \geq 1 - \delta\}. \quad (53b)$$

Let  $K = n - \sum_{i=1}^n J_i$  be the number of observed successes (i.e., observed  $J_i = 0$ ). First note that if we observed no successes i.e.,  $K = 0$ , then  $J_{(k)} \leq 0$  is impossible to achieve. Thus, in this case we are forced to take the trivial lower bound of  $\tau^* = 0$ .

Now, consider when we observe at least one success so that  $K > 0$ . Requiring  $J_{(k)} \leq 0$  is equivalent to  $k \leq K$ . Therefore, we may instead require that

$$\min\{k' \mid \text{Bin}(k' - 1; n, \tau) \geq 1 - \delta\} \leq K. \quad (54)$$

This condition is, by the definition of minimum, equivalent to instead requiring that

$$\text{Bin}(K - 1; n, \tau) \geq 1 - \delta. \quad (55)$$

Thus, the optimization in Equation 52 is equivalent to

$$\tau^* = \max\{\tau \in [0, 1] \mid \text{Bin}(K - 1; n, \tau) \geq 1 - \delta\}. \quad (56)$$

Note that (for  $K > 0$ )  $\text{Bin}(K-1; n, \tau)$  is continuous and monotonically decreasing with respect to  $\tau$ , reaching 1 as  $\tau$  approaches 0 and 0 as  $\tau$  approaches 1. Thus, by the intermediate value theorem, there exists a unique value solving  $\text{Bin}(K-1; n, \tau) = 1 - \delta$ . In particular, because  $\text{Bin}(K-1; n, \tau)$  is monotonically decreasing with respect to  $\tau$ , we can conclude that the solution to the optimization in Equation 56 is simply the solution to the equation i.e.,

$$\text{Bin}(K-1; n, \tau^*) = 1 - \delta. \quad (57)$$

By a similar monotonicity argument, we can conclude that  $\tau^*$  also solves

$$\tau^* = \min\{\tau \in [0, 1] \mid \text{Bin}(K-1; n, \tau) \leq 1 - \delta\}. \quad (58)$$

In particular, the solution will again lie at the boundary (Equation 57). However, by writing  $\tau^*$  as the optimization in Equation 58 we can also naturally cover the case where  $K = 0$  (in which case the optimization gives  $\tau^* = 0$ ). Furthermore, this aligns with our actual implementation which executes a bisection search to find  $\tau^*$ .

By construction,  $\overline{\text{VaR}}_{\tau^*} \leq 0$ . Leveraging the guarantee of Theorem 1, we know that

$$\Pr[\text{VaR}_{\tau^*}(J) \leq \overline{\text{VaR}}_{\tau^*}] \geq 1 - \delta. \quad (59)$$

Combining these facts,

$$\Pr[\text{VaR}_{\tau^*}(J) \leq 0] \geq 1 - \delta, \quad (60)$$

which, using the equivalence noted in Equation 51, implies

$$\Pr[p \geq \tau^*] \geq 1 - \delta. \quad (61)$$

Lastly, we transform from a lower bound on the probability of success to an upper bound on the probability of failure

$$p \geq \tau^* \iff q \leq 1 - \tau^*. \quad (62)$$

Thus, (61) implies

$$\Pr[q \leq 1 - \tau^*] \geq 1 - \delta. \quad (63)$$

Defining our probabilistic upper bound on the failure probability as

$$\bar{q} = 1 - \tau^* \quad (64)$$

concludes the proof.  $\blacksquare$

**Remark.** Although we derived  $\tau^*$  using our earlier VaR bound in Theorem 1, (58) takes the same form as the one-sided Clopper-Pearson lower bound [43, 49] which is known to be unimprovable amongst non-randomized approaches [49].

#### F. Proof of Theorem 5

Let  $\bar{P}$  be a finite-sample bound for performance measure  $\mathcal{P}(g)$  with error rate  $\delta$ :

$$\Pr[\mathcal{P}(g) \leq \bar{P}] \geq 1 - \delta \quad (65)$$

and consider the constraint

$$\mathcal{P}(g) \leq C. \quad (66)$$

For the test which accepts when  $\bar{P} \leq C$  we can upper bound the false positive rate as

$$\Pr[\bar{P} \leq C \mid \mathcal{P}(g) > C] \leq \Pr[\bar{P} < \mathcal{P}(g)]. \quad (67)$$

Then, by the guaranteed error rate of  $\delta$ , we get

$$\Pr[\bar{P} < \mathcal{P}(g)] = 1 - \Pr[\bar{P} \geq \mathcal{P}(g)] \leq \delta. \quad (68)$$

Combining, we obtain the desired bound on the test's false positive rate

$$\Pr[\bar{P} \leq C \mid \mathcal{P}(g) > C] \leq \delta. \quad (69)$$

$\blacksquare$

#### G. Proof of Theorem 6

Suppose we are given  $m$  policies  $\mathcal{U}_{1:m}$ , with unknown true performance  $\{P^{(i)}\}_{i=1}^m$  and associated probabilistic bounds  $\{\bar{P}^{(i)}\}_{i=1}^m$  individually holding with coverage level  $1 - \delta$  i.e.,

$$\Pr[P^{(i)} \leq \bar{P}^{(i)}] \geq 1 - \delta. \quad (70)$$

Let  $\bar{P}^*$  be the lowest probabilistic bound and let  $P^*$  be the associated true statistic i.e.,

$$i^* = \arg \min_{i=1:m} \bar{P}^{(i)} \quad (71a)$$

$$\bar{P}^* = \bar{P}^{(i^*)} \quad (71b)$$

$$P^* = P^{(i^*)}. \quad (71c)$$

First note that the probability of the minimum bound holding is at least as likely as all the bounds holding:

$$\Pr[P^* \leq \bar{P}^*] \geq \Pr[P^{(i)} \leq \bar{P}^{(i)} \forall i]. \quad (72)$$

Note that even though we do not assume  $\mathcal{U}_i$  are independent, we can assert the events  $P^{(i)} \leq \bar{P}^{(i)}$  and  $P^{(j)} \leq \bar{P}^{(j)}$  are independent for  $i \neq j$  as bound  $i$  is generated with different random samples than bound  $j$ . Applying independence yields

$$\Pr[P^{(i)} \leq \bar{P}^{(i)} \forall i] = \prod_{i=1}^m \Pr[P^{(i)} \leq \bar{P}^{(i)}]. \quad (73)$$

Each bound holds with probability at least  $1 - \delta$  so

$$\prod_{i=1}^m \Pr[P^{(i)} \leq \bar{P}^{(i)}] \geq (1 - \delta)^m. \quad (74)$$

Combining the steps, conclude that

$$\Pr[P^* \leq \bar{P}^*] \geq (1 - \delta)^m. \quad (75)$$

#### H. Proof of Theorem 7

Applying Theorem 6 with  $\bar{\delta} = 1 - (1 - \delta)^{1/m}$  we get final coverage

$$\Pr[P^* \leq \bar{P}^*] \geq (1 - \bar{\delta})^m = 1 - \delta. \quad (76)$$

$\blacksquare$